Politecnico di Torino

Master's degree in mechanical engineering
A.a. 2023/2024
December 2024

FUNCTIONALLY GRADED LATTICE STRUCTURES FOR STRUCTURAL APPLICATIONS: DESIGN, PRODUCTION AND PERFORMANCE ANALYSIS

Academic Supervisor:

Prof. Abdollah Saboori

Candidate:

Osman Gunaydin

Master Thesis

Summary

FUNCTIONALLY GRADED LATTICE STRUCTURES FOR STRUCTURAL APPLICATIONS:
DESIGN, PRODUCTION AND PERFORMANCE ANALYSIS

Osman GUNAYDIN

Politecnico Di Torino
Mechanical Engineering Master science
Supervisor: Prof. Abdollah SABOORI
2024,

Nowadays, functionally graded lattice structures have become popular due to their low weight and high strength. Additionally, flexibility of designing various layers and orientation made them very good candidates for bone implants. In this study functionally graded lattice types Gyroid, SplitP and Diamond were constructed into cylindrical geometry. The aim was to design a lattice structure which can provide similar relative density levels with the human bone, high strength and high load carrying capacity. Functionally graded lattice samples made of AlSi10Mg are printed by selective laser melting. Functionally graded lattice structures are evaluated by conducting quasi-static compression experiments. The effects of lattice structures on specimens' compression performance are investigated by analyzing surface morphology and deformation behavior.

Key Words: TPMS, density gradient design, SLM, Compression test

Acknowledgements

I would like to thank Professor Abdollah Saboori for the opportunity to conduct this thesis under his guidance. I also would like to thank Mohammad Hossein Mosallanejad and Mohammad Taghian for giving their endless support. Finally, I would like to thank my family and colleagues for their never-ending support throughout my master`s education.

Table of Contents

1. INTRODUCTION

From the first step to last, human and human body itself live in continuously movement state thanks to our anatomical and biomechanical structure. Humans state, humans subjected to not only static but also dynamic load conditions. Even though, human body is well adapted to these conditions, there is a probability of failure of bone structure in future life. Through the years biomedical sector has been working on implant technologies to imitate properties of human bone structure. However, this imitation requires certain types of performances such as ability to bone cell ingrowth, biocompatibility, gradient density variation etc. [1-3]. Recently, research has focused on finding replacement to conventional bone repair methods like autografts and allograft which can cause complications or require the right donors. Prosthetic alternatives for bigger bone areas exist but are expensive due to biocompatible materials and specific manufacturing requirements. Promising research is scaffold-based bone implant which possess porosity inside of the structure that can support bone growth through cellular adhesion. This phenomenon called "osteointegration" which is related with the biocompatibility of live bone tissue of the implant and consequently bone tissue repairs. Conventional strut based scaffolding applications have limitation in stress concentration and altering properties of the design. Newer works use surface-based structures such as Triply periodic minimal surfaces (TPMS). TPMS structures are derived from mathematical formulas. In literature, TPMS-based designs require high surface areas and strength such as load carrying scaffolds, static mixers and heat exchangers and in much research outweigh than traditional designs. In literature and engineering research, TPMS-based structures have shown unique results in many fields. For example, high hydrogen density, low pressure drops in catalytic substrates, acoustic isolation, high surface- volume ratio and so on. For biomedical fields, TPMS structures provide cell adhesion and mass flow with low-pressure drop-in bone tissue engineering. Also functionally grading their properties such as density the bone`s elastic modulus can be matched and stress shielding avoided. Meanwhile, uniform TPMS lattices are versatile, they don´t imitate the complex density transitions within human bone. This limitation can be improved by functionally graded structures where density varies directionally and can be further improved by topology optimization. To welcome complex loading cases, the implant structure required to be a varying in volume fraction, sequential layer collapse behavior and graded density. Therefore, Functionally Graded (FG) structures are offered not only as a particular structure but also as a broad meaning of topological or geometrical grading. Functionally Graded (FG) structures are also widely used in aerospace, nuclear energy, defense and tooling industries.
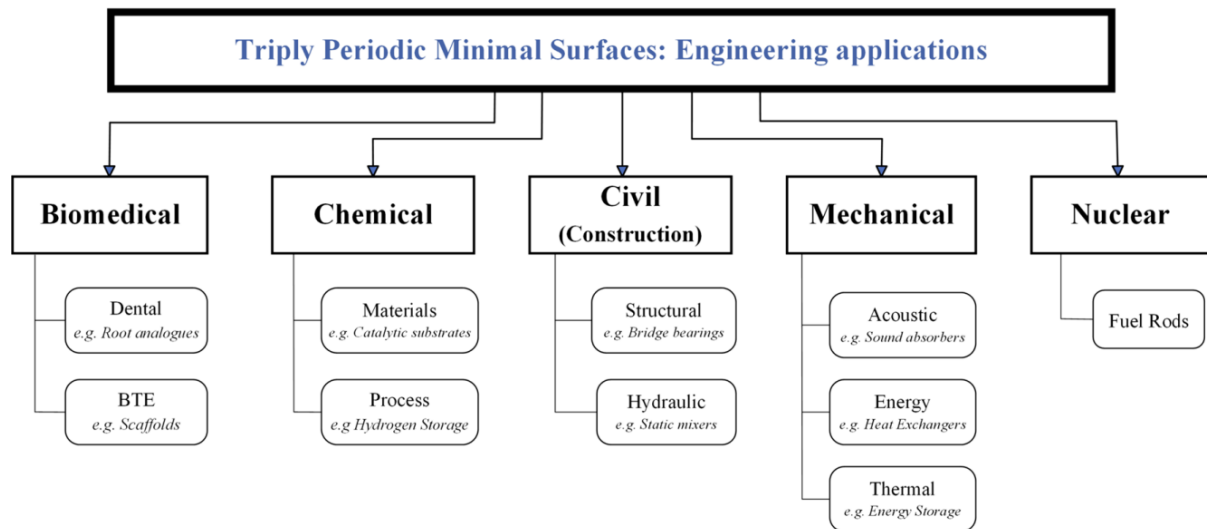
Figure 1. Summary overview of TPMS applications [47].

Recent advancements in additive manufacturing (AM) have caused the cost-effective manufacturing of complex structures. Although conventional manufacturing methods are widely in use, their limitations of constructing complex geometry, environmental impact and high energy consumption made them inferior against AM technologies. Additionally, their compassion was investigated in many research and AM parts found better in terms of energy absorption, uniformity of microstructure [3-7]. AM can provide manufacturing of metal components and periodic lattice structures thanks to Selective Laser Melting technologies. thanks to high cooling rates, fine surfaces (15-80 μm) and high strength, Laser Powder Bed Fusion (L-PBF) method implemented. As powder material AlSi10Mg used due to good mechanical strength, adequate hardness, and dynamic properties as well as low weight [8,9]. The generation of STL files were created by using nTop (nTopology, New York, NY, USA). In addition, 6 various Triply Periodic Minimal Surface (TPMS) lattice structure modelled, and density gradients applied through lattice structures. After design and production steps, the surface state had been investigated via Optical Microscope (OM). In addition, mechanical performance analysis is completed via quasistatic compressive test instruments. The last but not least homogenization approach implemented to compare and analysis behavior of single unit cell.

The aim of this study is investigating FG lattice structures and their performance analysis regarding design, production and mechanical performance. After the result of this study, it is expected that by imitation of density gradient in human bone can be applied to metal components and their performance can be a good candidate for biomedical applications.

2

1.1. Additive Manufacturing

Additive Manufacturing (AM) is a manufacturing process of joining materials to make objects from 3D model data via adding layer by layer. AM was born with the name "Rapid Prototyping" (RP). RP was invented in the 20th century. RP is used to explain the process that makes a prototype of final product before the industrialization stage. The result of this process was investigated and tested to create accurate models and consequently the final product. It was the first method that allowed to create 3d object from CAD model.

This was the first step. Afterwards, AM has grown a lot, and it is used in many fields. Rapid prototyping term is no longer exists since it is unnecessary to explain the concept of the process. Especially, this manufacturing technique, allows industry for design of new parts and tools. However, the AM method's greatest benefits still lie with small batch production. Due to its high machine and job time. Nonetheless, AM can affect the cost and job time as shown in the graph.
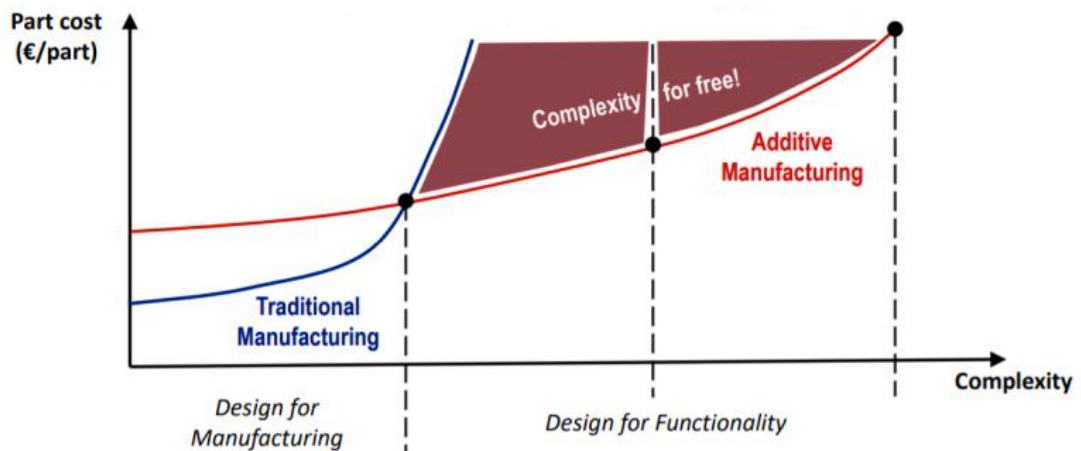
Figure 2. relation between. part cost and complexity for AM and others [47].

AM is very advantageous not only for prototyping but also for complex geometries. AM can provide the ability to create specific shapes and internal surfaces that would not be possible with conventional techniques [48].

As above-mentioned paragraph the first name of the AM was rapid prototyping. The man who patented this was the Japanese Hideo Kodama from Nagoya research industry in 1980. However, due to economic problems, he couldn´t take full patent. Couple years later in 1985, French electrochemical engineer who is Alain Mehaute invented the stereolithography (SLA) process. Meanwhile, Chuck Hull from the USA patented the same process and set up a 3D printing system to commercialize this discovery. The first product of SLA was commercialized in 1988. In SLA, thanks to UV light materials like liquid resins, photopolymers can be turned into solid to create parts. Therefore, nowadays Chuck Hull is known as the father of the SLA. In addition, stereolithography name was given to the file format for the AM which is "STL file". Afterwards, Carl Deckard from the USA created the Selective Laser Sintering (SLS) process for reducing costs and time in the machine industry. Meanwhile, Scott Cramp also was designing a machine that could print 3D parts. By mixing the was with polyethylene he printed 3D parts. After printing the couple of toys, he realized that this process could be automated. Thus, "Fused Deposition Modeling" (FDM) discovered. Later, AM processes became popular. At the end of 20th century SLS and FDM technology find its place in the Europe market. In seven years, the market had increased and lots of companies invested in AM processes such as Selective Laser Melting (SLM) and Binder Jetting (BJ). Thanks to this rapid growth of the market, cad tools for 3D printing developed and became available for its users. Also, some medical research had been conducted in the nineties which lead to endless options for the medical industry. Early years of 21st century also was key time for AM. Due to, organ replacement in medical field market had grown a lot [48].
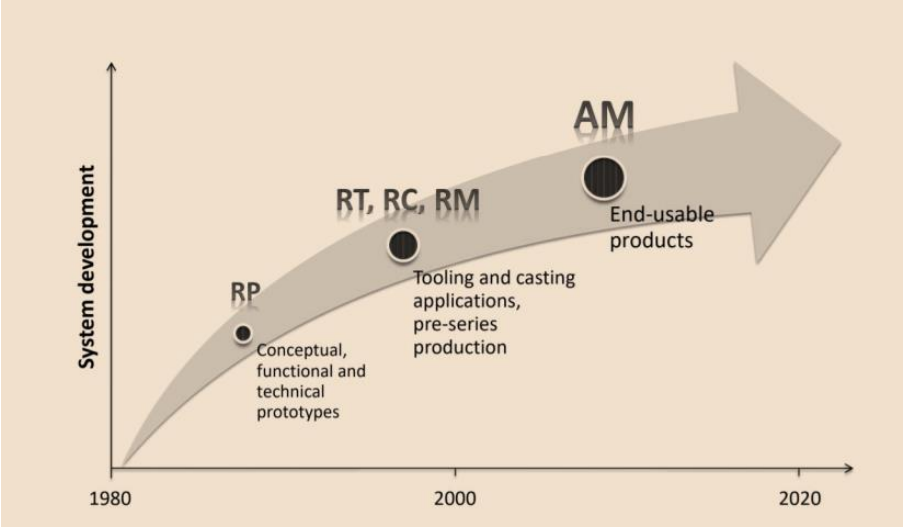
Figure 3. system development of AM [47]
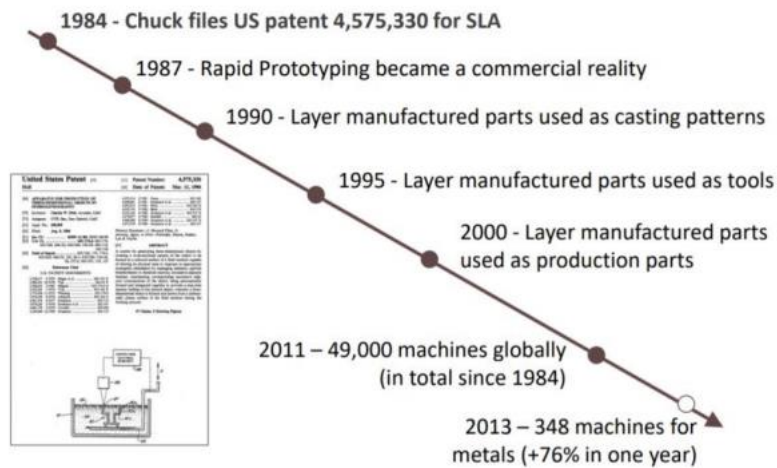
Figure 4. history of AM [47].

Despite conventional manufacturing methods, AM process requires solely some basic dimensioning, material and a small amount of operational knowledge regarding printing machine. A major advantage of additive manufacturing is ability to print parts with complex geometrical surfaces. This ability provides almost free design possibilities and precise control over not only external but also internal structures. This advantage has fundamentally evolved into final products from the way components are designed. The key advantages of additive manufacturing include:

- The ability to generate smaller parts with complex topologies which can be challenging to reach using conventional methods.
- Minimal waste and material efficiency which leads to environmental benefits.
- The possibility of reducing part mass by including material for only specific properties.
- Ability to facilitate simpler assembly processes by decreasing the number of machine elements.

AM has become more famous over the past few decades due to increasing request for complex, high special components. AM often requires only 3D model to produce a almost finished part. Between 2010 and 2015, additive manufacturing related research and development reached 30% annual growth. AM is now becoming more applicable across nearly all industries. These sectors are mainly automotive, mechanical, medical implant and aerospace with a specific focus on producing lightweight structures which offer high performance at decreased cost. This change has gained attention in manufacturing technology

for cellular materials, which combine high strength with strong impact resistance and energy absorption characteristics [34].

Basically, it works layer by layer according to Computer Aided Design (CAD) data and the way of creation, thickness of layer plays crucial role in quality of printed parts [10]. AM process have 8 steps:

1. CAD
2. STL convert
3. File transfer to machine (g-codes)
4. Machine setup
5. Printing
6. Part removal
7. Post processing
8. Application
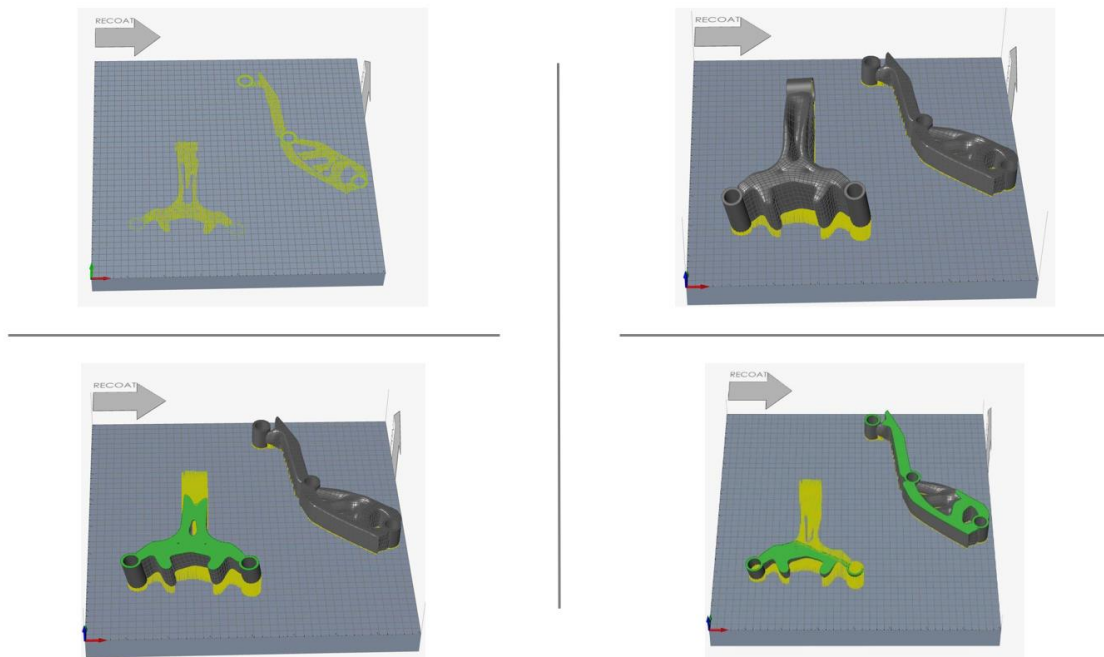
Figure 5. Slicing procedure of some parts for automotive field.

1.1.1. Powder Bed Fusion Process

Powder bed fusion (PDF) is a process in which thermal energy selectively fuses regions of a powder bed. All PBF methods share a basic characteristic such as one or more thermal energy sources to induce fusion between powder particles. However, as an energy source Laser Powder Bed Fusion (LPBF) laser, Electron Beam Melting (EBM) high intensity

electron beam is being used. These methods are also called Selective laser melting (SLM) processes. Basically, specific areas of the powder bed are scanned along predefined lines thanks to energy source. The heated region which is substrate is cooling down and solidifies, forming a new layer of product. After initial layer formation, the powder rack moves upward to spread new material required to print the new layer. The building platform lowers down which equal thickness of new layer, and rack transfers the powder to the melting zone to build new surfaces. The same step continues until the final layer is obtained. Even though PBF methods are widely implemented in research where high strength and energy absorption performances are required, they are expensive and are not well adapted for mass production [11,12]. However, to design complex shape and graded lattice formation makes these methods superior then other conventional manufacturing methods.
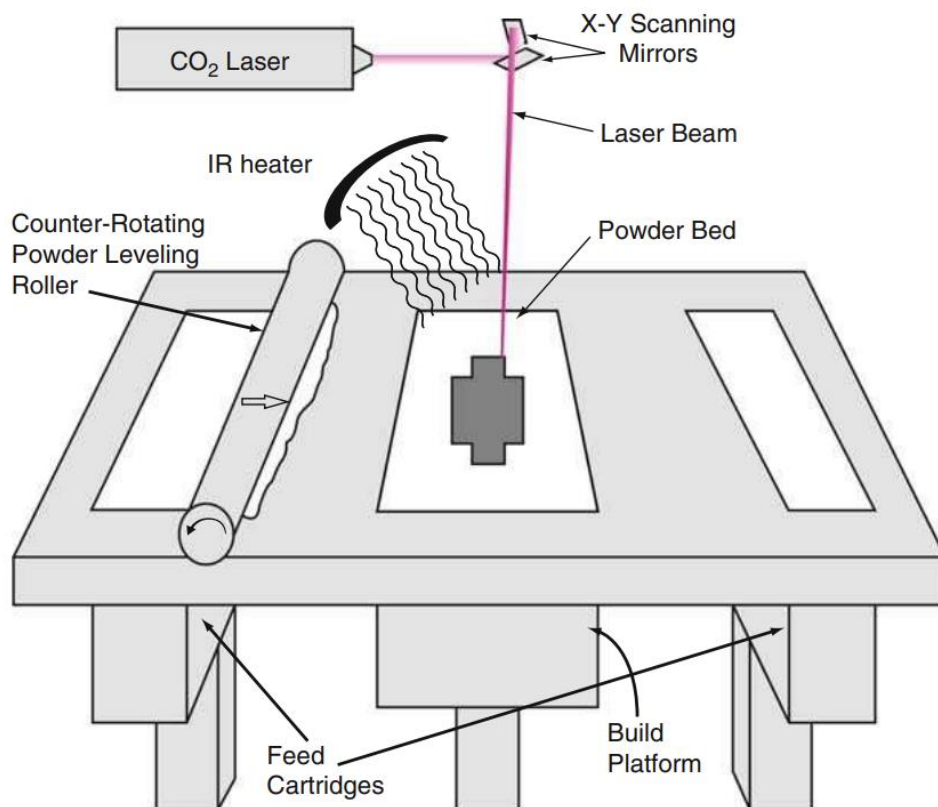
Figure 6. Schematic of PBF process [10]

1.1.1.1.   Electron beam melting

The electron beam melting (EBM) process directs a high energy electron beam to melt metal powder particles for AM. This technique takes place in a high vacuum environment to prevent oxygen involvement into the manufacturing process. In electron

beam melting, metal powders are put into build volume and melted by machine-controlled beam source. This process temperature can increase up to 1100 degrees. The cooling rates during EBM can vary from 10^2 to 10^3 K/s to enable control on solidification parameters like the thermal gradient. By adjusting the electron beam`s position, speed and current, it's possible to affect the cooling rate which in turn affect the grain size. This provides heterogeneity for nucleation and refines grain structure along solidification area. Finally, EBM has major advantages including low residual stress and oxidation in the final product [43].
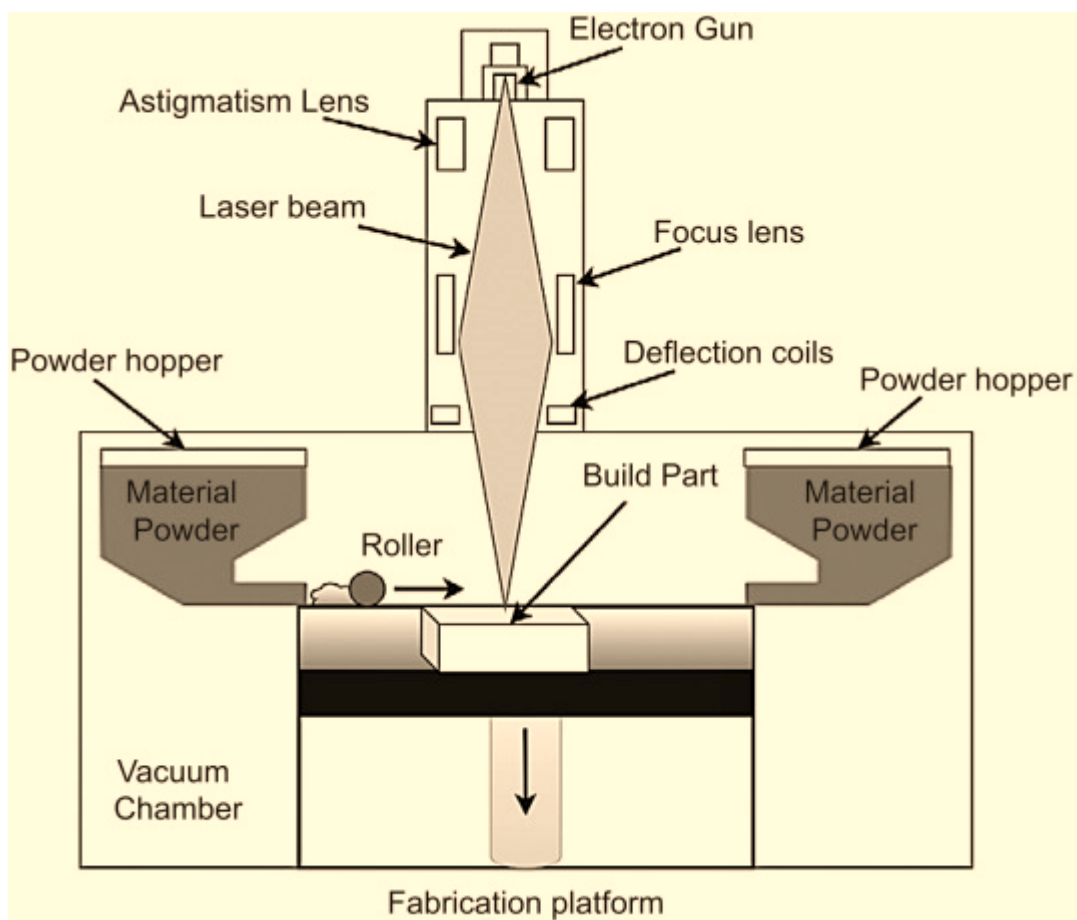
Figure 7. EBM process [44].

1.1.1.2.   Laser Powder Bed Fusion

Laser powder bed fusion (LPBF) melts the metal powder with laser beam. This technique involves expanding a thin layer of powder on the build chamber. Unmelted powder in the build chamber provides supports parts as they are built. After each layer

cools down, the build platform lowers down, allowing a new layer of powder to be expanded and melted on the previous layer. Cooling rates can vary from 10^3 to 10^8 K/s and this rapid cooling rate can affect finer grain structure. LPBF is highly advantageous for complex parts, also supports a wide range of materials and mostly requires low number of supports. It provides efficient approaches for fabricating intricate gradient structures [44].

1.1.1.2.1. Aluminum Alloys for PBF

Nowadays, the most used Aluminum alloys for LPBF are based on Al-Si foundry alloys as the Si-based eutectic provides perfect castability and manufacturability. But these alloys typically reach 150-300 MPa and therefore don´t meet expectations for higher strengths. Higher strength materials are beneficial by increasing potential for load bearing, light-weighing and cost savings. However, it's evident that major challenges are linked to development of high strength aluminum alloys in LPBF. Additionally, printability and defects were critical issues. Nevertheless, some strategies have been introduced into research field and these challenges were outcome by science. For example, designing new alloys for specific LPBF applications and adaptation of existing high-strength alloys to LPBF [49]. To summarize Aluminum alloys for LPBF:

- They´re know with their lightweight and cost effective
- Good strength, hardness and thermal properties which become good candidates for many fields
- Good post process finishing
- Excellent corrosion resistance and low density

Figure 8. Engine tank printed with AlSi10Mg [50].

1.2.   Cellular Materials

Cellular solids are formed up of an interconnected network of solid struts or plates which form the edges and faces of cells. The simplest example of cellular material is honeycombs in which hexagonal cells of the bee. Basically, the cells are polyhedral that pack in 3d cellular material foams. If the cell is only made by cell edges the foam is called open-celled. If the faces are solid too, it becomes closed-cell geometry. The most important property of a cellular material is its relative density which is the ratio between density of cellular and bulk structure. Generally, all materials can be foamed. These are mainly polymers, metals, ceramics etc. Usually, cellular solids have relative densities lower than 0.3. Additionally, the cell size is another important parameter which can affect mechanical and thermal properties of the material. Cell shape is also another important parameter; when the cells equiaxed type the properties are isotropic [13].

1.2.1. Cancellous Bone

Most bones possess a very detailed structure. It consists of compact bone and a core of porous cellular which is called cancellous or trabecular bone. Due to aging through time, to avoid loss of mass of cancellous bone, artificial hip implant widely applied. As it can be seen in the figure, the cellular structure of cancellous bone is made up of an interconnected network of rods.
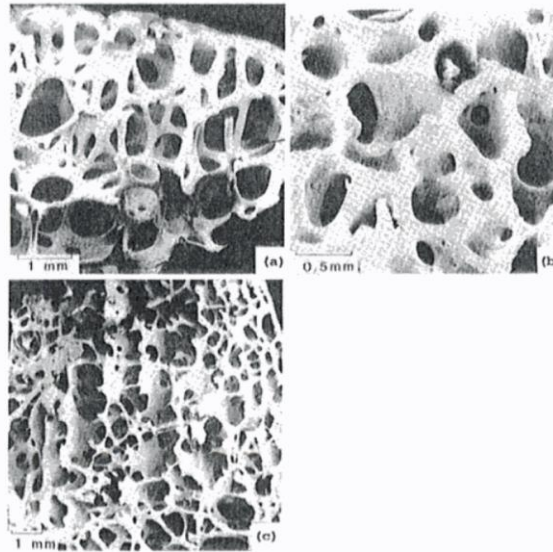
Figure 9. Cancellous bone [13].

Figure 9. SEM images show the cellular structure of trabecular bone. (a) Sample derived from the femoral head, showing low-density, open-cell, rod-like structure. (b) Sample derived from the femoral head, showing a higher density, perforated plate-like structure. (c) Sample derived from the femoral condyle, of intermediate density, present an oriented structure, with rods normal to parallel plates.

In literature, the relative density of cancellous bones differs between 0.05 to 0.7. Additionally, the relative density of bone which is less than 0.7 classified as "cancellous "[13].

2. Lattice Structures

2.1. Functionally Graded Lattice Structures

Lattice structures are porous type structures that combine 3D unit cells periodically with a certain relative density which is the ratio between cellular and bulk structure. Lattice structures are also known for their good performance in topology, manufacturability and stiffness. Relative density is a key parameter in the design of lattice structures and the main variable used to control lattice features by gradient density. The example of uniform lattice structures is various such as bamboo, beetles and fish outer skin etc.
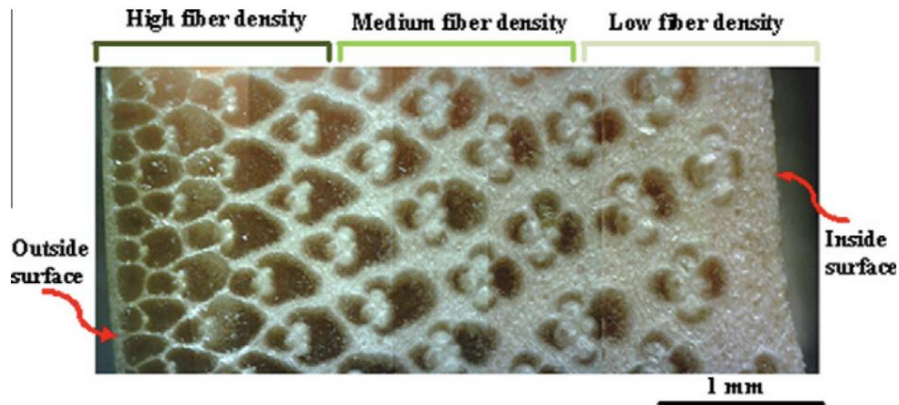
Figure 10. Lattice structure of bamboo [16].
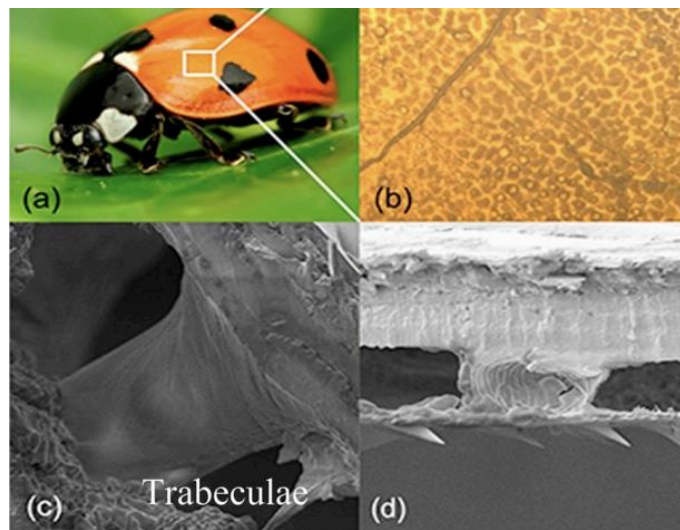
Figure 11. Ladybeetle forewing microstructures [17].

However, when requirements vary from case to case, adaptation of these lattice structures according to performance becomes crucial. Functionally graded lattice structures (FGLS) are non-uniform lattice structures designed with a density gradient ordered by given function whether that can be mechanically or thermally and biologically. FGLS play an important role in innovative manufacturing technologies. Due to its tunable and customizable properties FGLS are extensively used in AM sectors [15-16]. Thanks to advance progress in design software computation expenses for exploring new geometries with materials have lowered. FGLS provides multiple options for reducing the number of elements in assembly while decreasing weight and manufacturing expenses.

The arrangement of density gradient to specific regions of the lattice enables optimized structures which can effectively respond to loads, high strength and stiffness. Additionally, FGLS can also be tailored for localized deformation of lattice layers from lowest density layer to the highest. Furthermore, they can be designed for mimicking microstructure of cortical and cancellous bones due to ability of both dense and highly porous regions in geometry [18].

2.1.1. Triply Periodic Minimal Surface (TPMS) Lattice Structures

Triply periodic minimal surfaces (TPMS) are surfaces with mean curvature of Zero and periodic structures in x-y-z coordinates [19,20]. TPMS structures have shown to be a versatile candidate of scaffolding and possess good stress distribution under loading due to its geometrical features [20-22]. Therefore, TPMS are considered as promising biomaterial lattice structures for future research. TPMS structures also have self-supporting features that do not require build of support in SLM technology [24]. In literature, it also mentioned that mean surface curvature of TPMS structures is also like the trabecular bone structure.

Furthermore, a study suggests that TPMS- based biomaterials are promising for improving tissue regeneration performance. Therefore, TPMS structures have been widely studied via AM technology.

In one research study, TPMS-based biomaterials (i.e. primitive, gyroid and diamond) each of structural porosity evaluated in terms of their mechanical properties, fatigue performance. It was found that some TPMS structures exhibit ideal performance of elastic modulus and yield strength of trabecular bone. Additionally, permeability for tissue regeneration was in range within bone structure [25].
Some TPMS structures are:
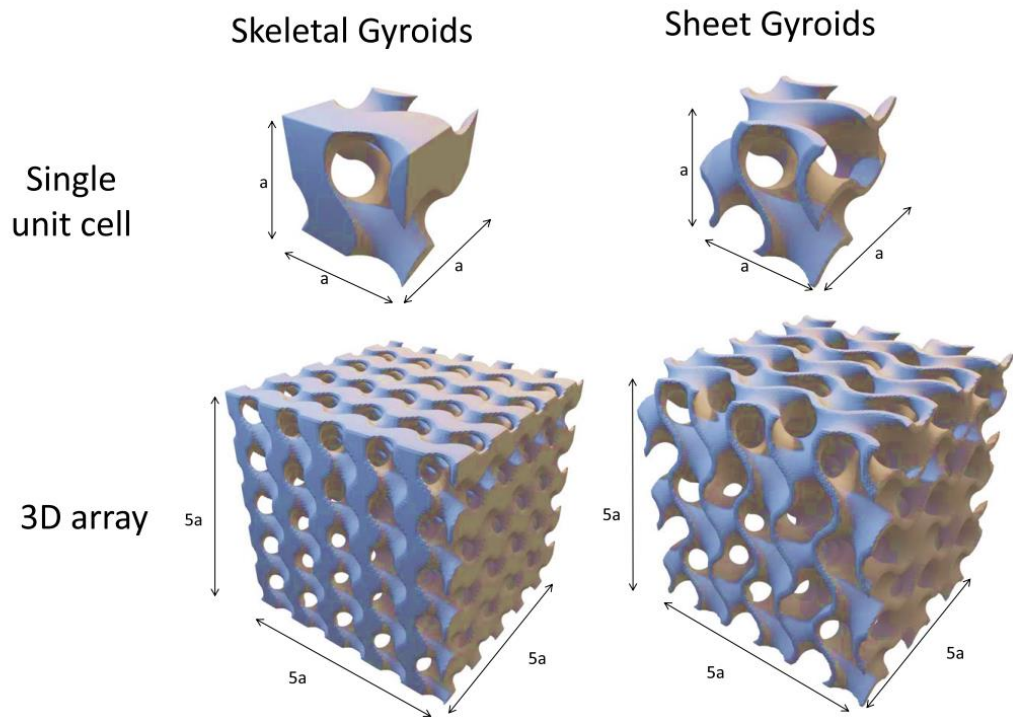
Figure 12. single Gyroid unit cells and 3D volume [26]
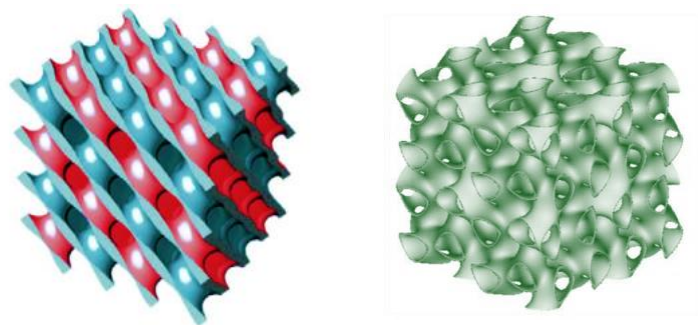
Figure 13. Diamond and SplitP TPMS structures [26,28].

3. STATE OF ART

To understand the behavior of lattice or cellular materials, first it must be clarified which parameters are involved in the study and their effects on the cell.

There are 3 variables: these are material, elative density and cell topology or shape [29]. To be identified as a cellular solid, relative density must be lower than 0.3 [13]. Shape and cell topology are related with the understanding of the mechanical response of lattice structures.

There are two types of response exist which are bending-dominated and stretch dominated. As it can be seen in the figure 7 below M is the Maxwell number which represents a basic form of prediction of mechanical behavior of the lattices.
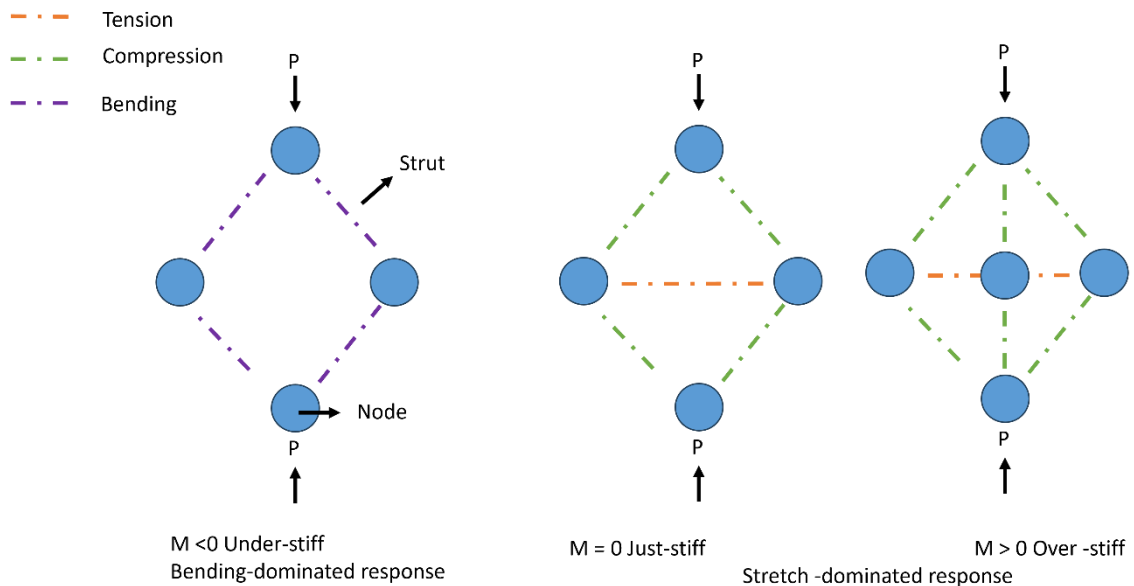
Figure 14. Stretch-dominated and bending-dominated structures [14].

The selection of one of these topologies depends on the preferred performance for the lattice and the features of material for manufacturing. However, the response of the lattice structure is mainly representative of stress-strain curves.

As can be seen in the figure below, there are three main stages that represent behavior.

1. Linear elastic region characterized by young modulus (E)

Deformation in this region is mainly due to bending struts.

2. Plastic region

Material exhibits plastic yielding and long collapse plateau. This can be attributed to the creation of plastic hinges at the nodes. If the material is brittle this region will fluctuate due to brittle fracture [30].

3. Densification region

Simply, the bending – dominated lattice will have large plateau stress, a big area in which stress being constant and increasing strain. This region also represents energy absorption behavior (good for protective equipment) of the structure until the failure. Considering stretch – dominated structure, the curve shows a higher yield strength. Additionally, deformation mechanism will be only tension and compression modes. Therefore, stretch – dominated lattices are adequate for light – weighting and bending dominated lattices more suitable for energy absorption [24,30].
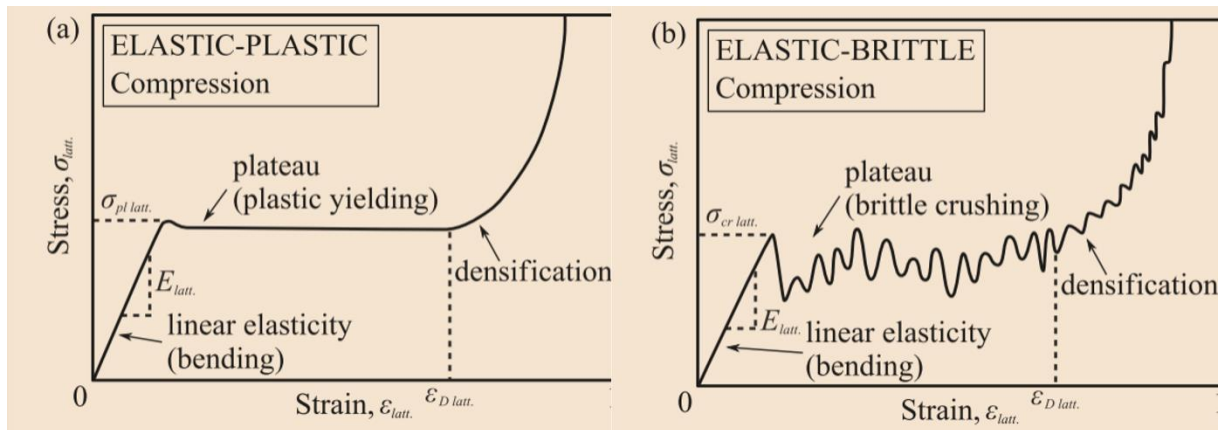
Figure 15. Compression behavior of bending-dominated (a) and stretch- dominated (b) lattice structures [30].

3.1.   Literature

When the literature researched regarding the functionally graded lattice structures, it was realized that there are several research which focus on crashing response, energy absorption performance, mechanical and failure models etc.

The FGLs mainly designed such as:

1. Density grading along parallel or perpendicular to building direction
2. Same density values but different unit cell size
3. Uniform structure comparison with thickness graduation and void size graduation
4. Relative density variation from inside to outside is like cancellous bone structure.

16

In 2019, Gyroid cellular structures with grading density along different directions had been investigated and manufactured by SLM. Samples were designed with density grading parallel and perpendicular to the building direction and their mechanical performances under compressive loading were compared with uniform lattice structure.
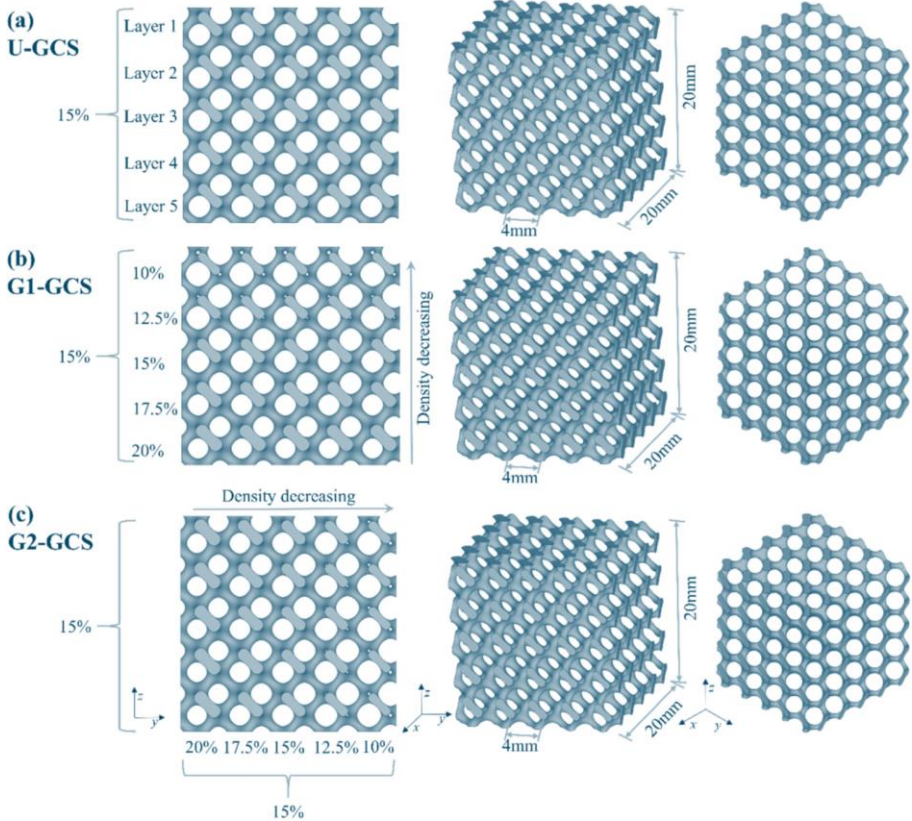
Figure 16. The images of (a) uniform Gyroid unit cell, (b) continuous Gyroid with the gradient along z axis, and (c) continuous Gyroid with the gradient along y axis [31].

It had been stated that cellular structures with density gradient perpendicular to building orientation exhibited similar deformation to uniform unit cellular structures. Additionally, perpendicular graded density increased the strength of the material. Another important result was structures with density graded parallel to building direction had distinct layer-by-layer collapse failure. Additionally, they also provided a large strain resistance before densification region reached [31].
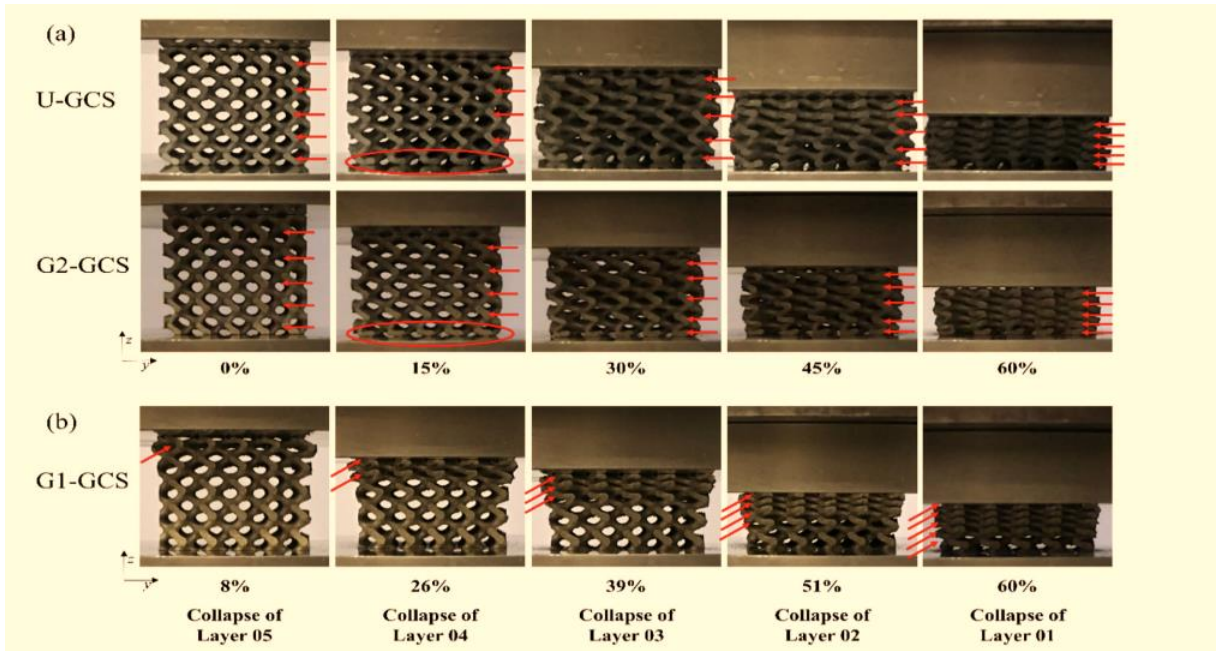
Figure 17. Layer by layer collapse behavior

In another research, compressive failure modes of double gyroid structures with different cell size compared. It had been stated that cell size played a crucial role in the failure mechanism of metal AM lattices. Furthermore, small cell size structure had better performance against low-strain failure caused by crack propagation.
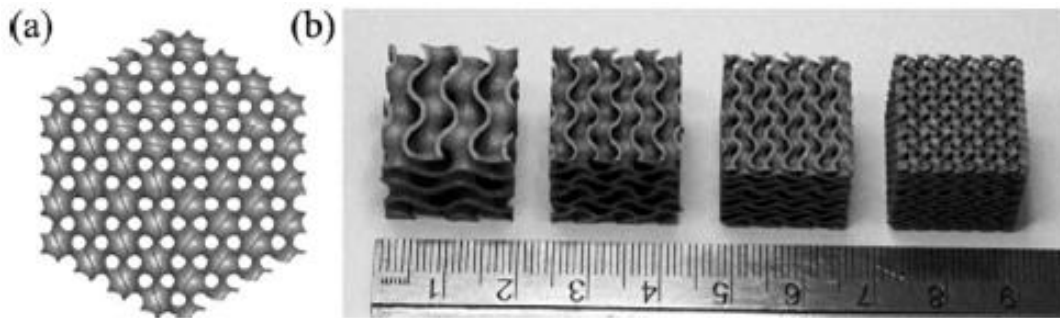
Figure 18. 3D model of the gyroid lattice (a) and pictures of AlSi10Mg SLM manufactured specimens (b). The specimens in (b), from left to right, contain cells of size 9, 6, 4.5 and 3 mm [32].
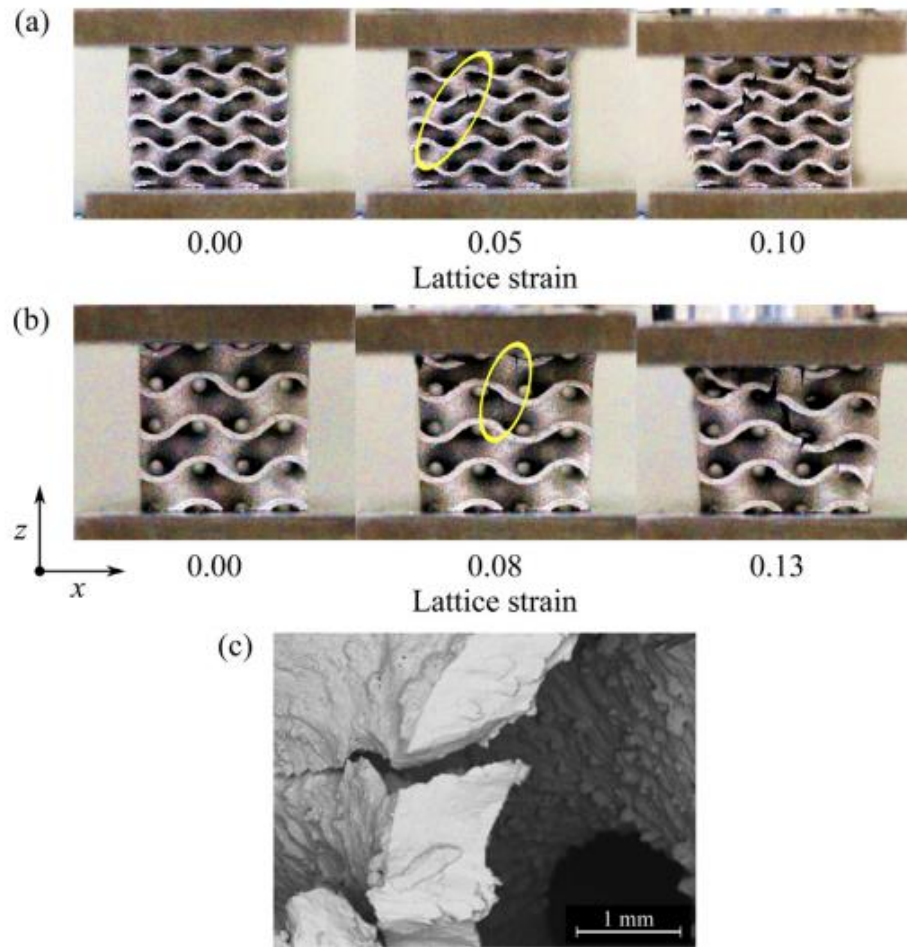
Figure 19. Crack initiation and propagation [32].

In 2022, 3d gyroid structured fabricated by EBM. Therefore, morphological and mechanical characteristics of samples were investigated. Samples mechanical properties were tested with quasi static compressive test machine. Consequently, deformation mode of cylindrical samples was similar, and they had shear bands with 45-degree angle. This result is also attributed as barreling effect which means phenomena by friction between sample and platen [45].
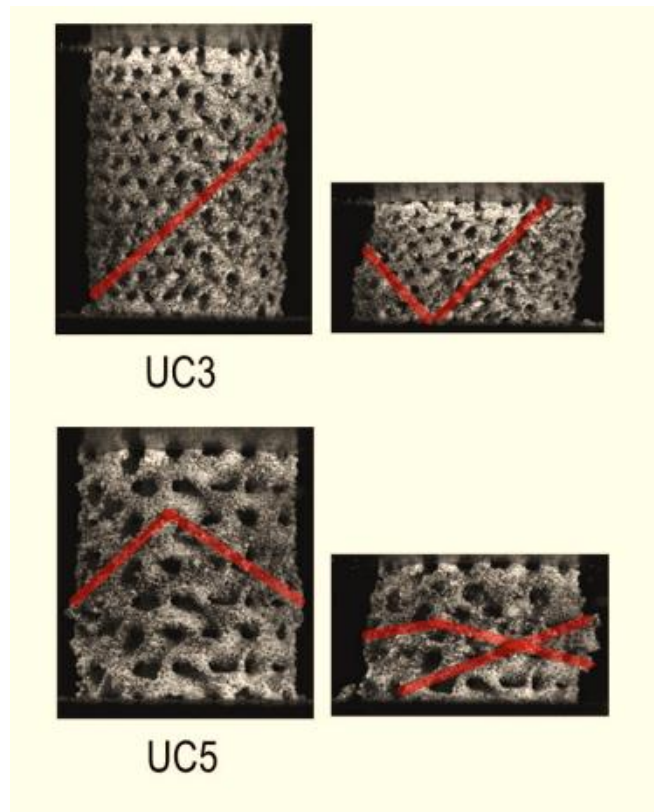
Figure 20. Representative failure behavior of samples [45].

Another research had been conducted in 2022. In this work, there were three different 17-4 PH gyroid lattice design procedures i.e., thickness graded, size graded and uniform. Mechanical performance and energy absorption performance under uniaxial compression test were compared. As a result, it was stated that uniform structure had better mechanical performance than graded ones.

Furthermore, some defects were detected in thin-walled regions within graded samples. However, graded samples had layer-by-layer collapse behavior and consequent light weight. Therefore, it had been found that this result was relevant to bending-dominating behavior and it sustained larger strain than uniform samples [33].

	15% density	25% density
U		
SG		
TG		
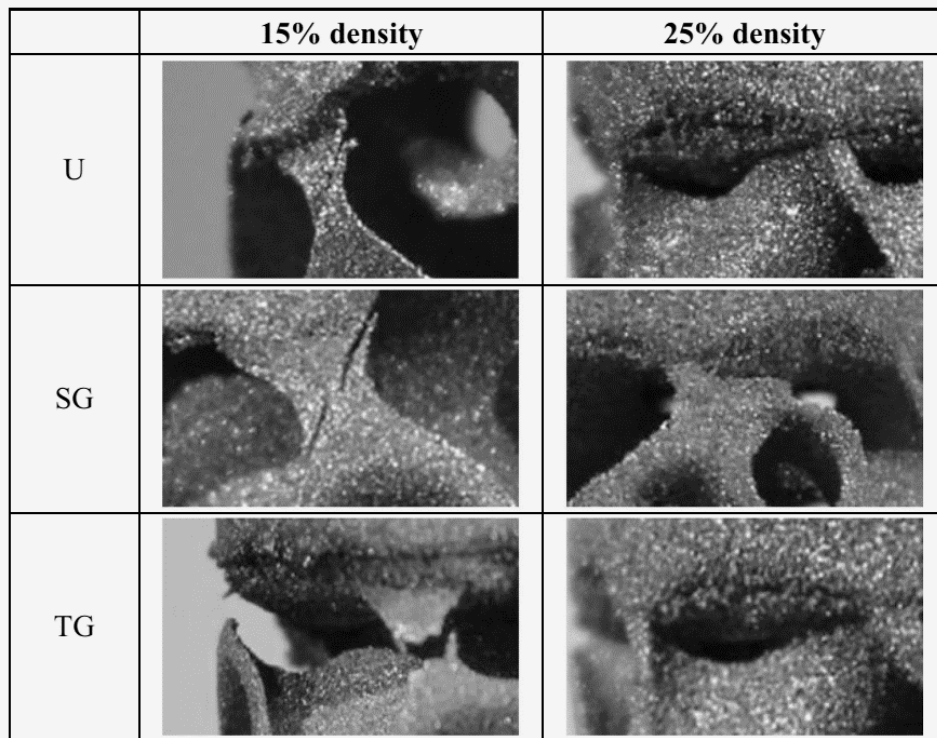
Figure 21. Defect analysis of the gyroid structures [33]
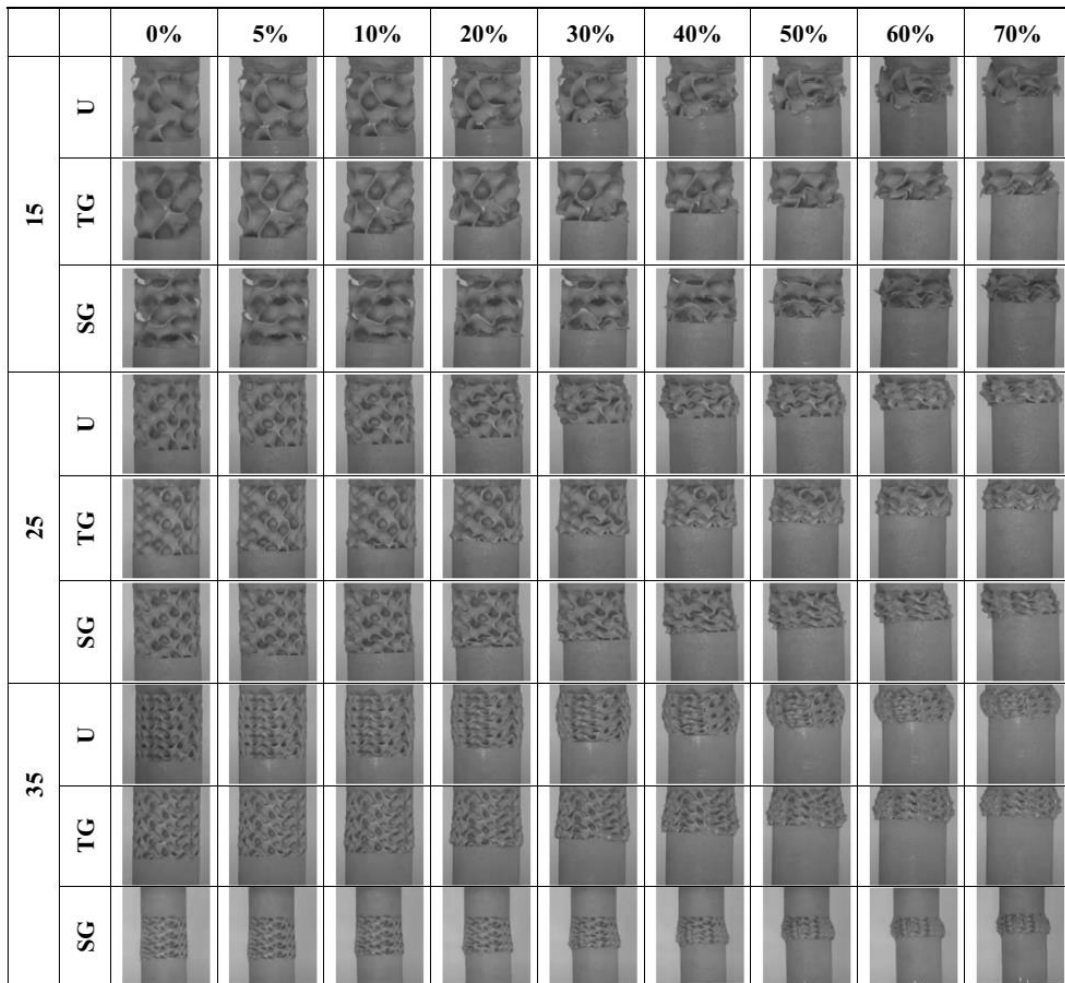
Figure 22. layer-by-layer collapse behavior of samples [33].

In another research, they studied hybrid and functionally graded novel designed cellular lattice structures and their mechanical properties.
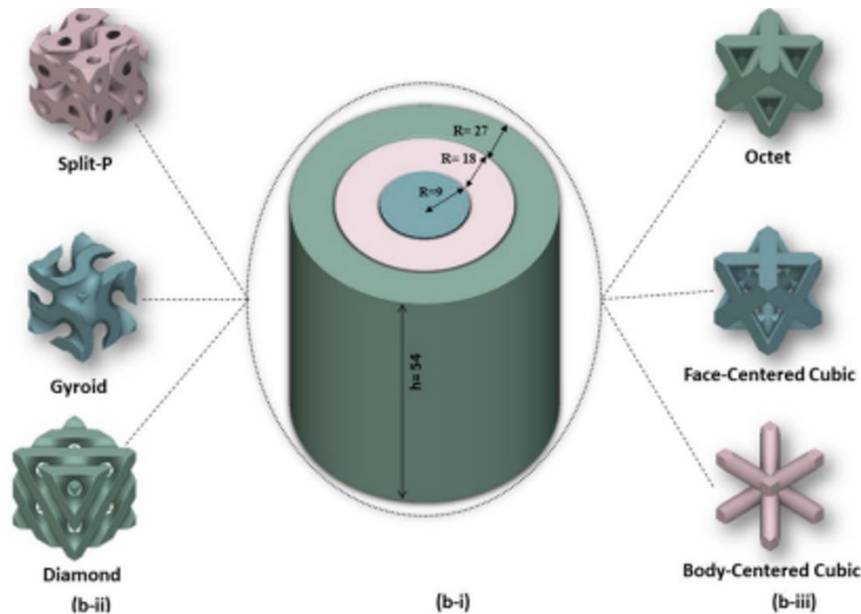
Figure 23. Three cylinders with different radius and the same height (b-ii) Three surface-based unit cells (names are shown on the figure), and (b-iii) Three Beam-based unit cells [34].

The novel design consists of cylindrical hybridization approach by merging three different unit cells: body-centered (BCC), face -centered (FCC) and octet from beam-based structures and gyroid, splitp, diamond from surface-based structures. These models were divided into hybrid and functionally graded lattice structure (gradient based) subcategories.

The difference between the subcategories were mainly in hybrid models only cell types were changed. As a variant for FGLs were thickness and unit cell sizes. Additionally, Polylactic acid (PLA) was used as material and fused filament deposition selected for AM process.

Afterwards, compression tests were conducted to evaluate ultimate strength, specific energy absorption and failure performance. Consequently, it had been stated that functionally graded lattice structures, if surface based or beam based or not showed improved mechanical performance than hybrid lattice structures. These were attributed to the effect of unique design. Another important result was varying mechanical performances of beam-based FGLs. While ultimate strength increased in the first model, it decreased for second and third. So that this was explained an effect of positioning of the unit cells, relative density and the buckling phenomena [34].

The last but not least, in 2021 researchers investigated mechanical behavior of TPMS cellular structures (Diamond, Gyroid, IWP, and Primitive) which were printed by the powder bed fusion technique using stainless steel 316L powder and conducted compression test with different loading velocities. Also, dynamic deformation characteristics were captured by using infrared thermography. Consequently, samples undergo strain softening (hardening) which means deterioration of strength with increasing strain in continuous loading [46].
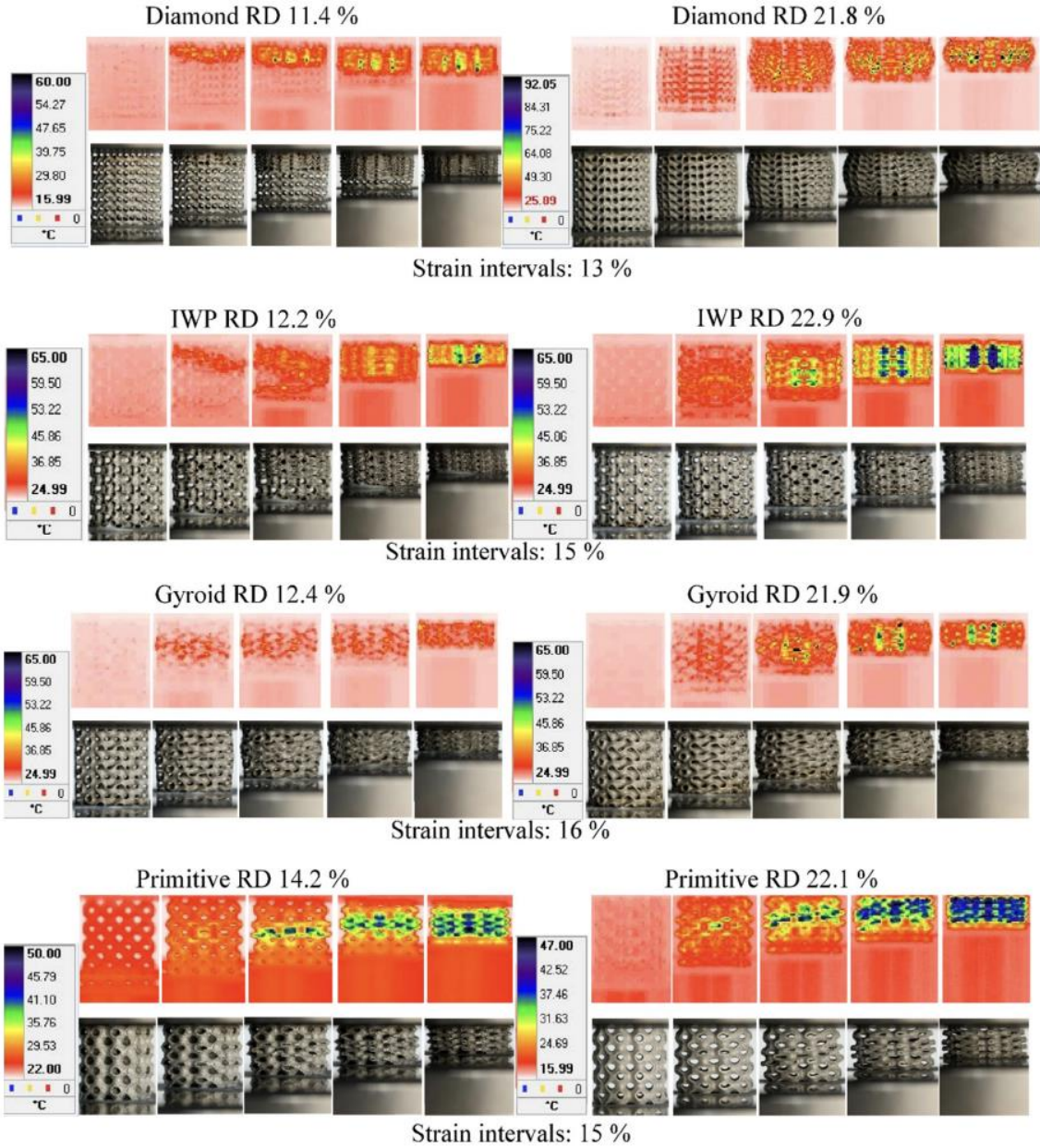
Figure 24 Deformation modes of TPMS specimens [46].

3.1.1. Numerical Simulation Theory

To predict the behavior of lattice structures, simulation methods are frequently implemented into studies. One and most famous one is The Finite Element Method (FEM). FEM is generally implemented to investigate mechanical performance of solid models. Even though it can provide accurate simulation results, it requires a complex and time-consuming meshing procedure. As complexity of the part increases, the computational efforts rise dramatically, especially for the lattice structures where the number of elements scale up with n^3

By treating material as an infinite medium and evaluating microscopic behavior of the unit cell, it is possible to define material performance at macroscopic level. This method is called homogenization [24].

Multiscale modeling is an approach where the analysis of material is conducted at one length scale, however the results are connected to various material features at a different length scale. Homogenization methods reduce significant savings in computational time. Additionally, in composites there is no need to model the whole structure of the composites. Homogenization can be also applied to lattice materials by simplifying the assumption where the lattice presents one phase [41].

4. MATERIAL AND METHOD

4.1. Design of Lattice Structures

In this procedure, FGL models were constructed via Ntopology software. Before setting dimensions for the models, human bone was taken as an example in terms of volume fraction variation as in figure below. Furthermore, as it has been stated in the literature relative density values were set to in range with cancellous bone which is around 0.4 to 0.8 g/cm³ [35]. As it can be seen in the figure below, cancellous bone has spongy like, and its volume and porosity vary from core to the outer shell.
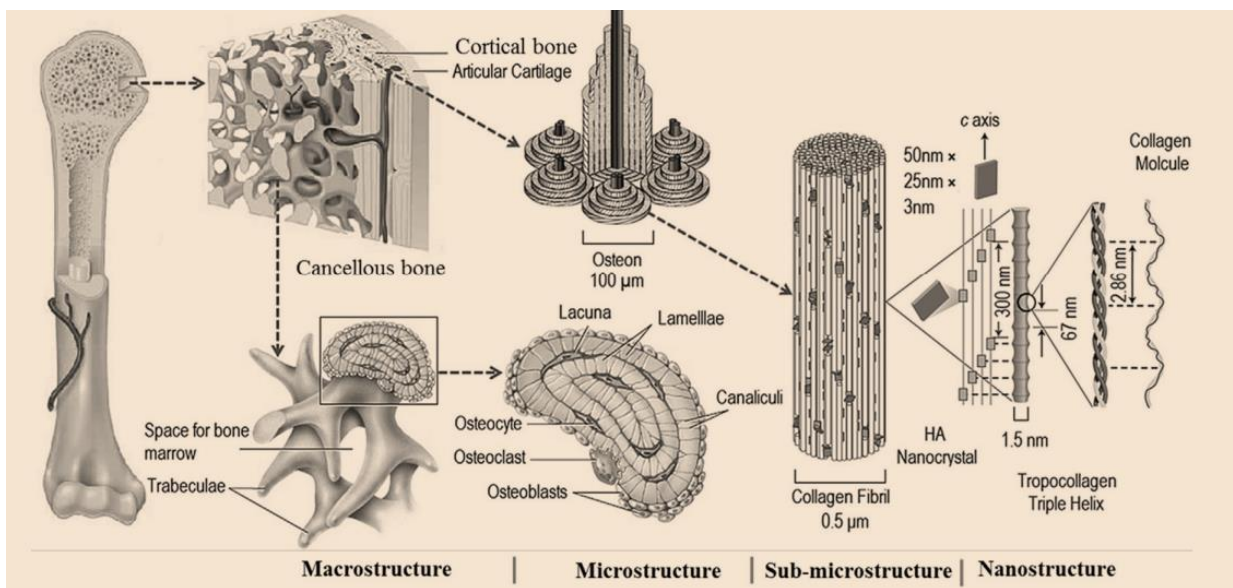
Figure 25. Inner structures of human cortical and cancellous bone [36].

Totally six cylindrical FGLs models were built. These consist of three different layouts of Splitp, Gyroid and Diamond structures. The rest of the models were built fully Diamond, Gyroid and Splitp. Additionally, cell sizes were kept constant for every sample. Furthermore, little off-set values were implemented to facilitate the merger between intersect cylinders.

1st sample	Cell type	Cell size (mm)	Radius (mm)	Relative density	Height (mm)
	Split P	10x10x10	2,6	0,705	
	Gyroid	9x9x9	5,6	0,448	
	Diamond	10x10x10	10	0,419	
2nd sample	Split P	10x10x10	2,6	0,708	
	Diamond	9x9x9	5,6	0,531	
	Gyroid	10x10x10	10	0,346	
3rd sample	Gyroid	10x10x10	2,6	0,492	
	Split P	9x9x9	5,6	0,528	
	Diamond	10x10x10	10	0,386	
4th sample	Gyroid	10x10x10	2,6	0,492	25 mm
	Gyroid	9x9x9	5,6	0,448	
	Gyroid	10x10x10	10	0,346	
5th sample	Diamond	10x10x10	2,6	0,617	
	Diamond	9x9x9	5,6	0,531	
	Diamond	10x10x10	10	0,419	
6th sample	Split P	10x10x10	2,6	0,708	
	Split P	9x9x9	5,6	0,580	
	Split P	10x10x10	10	0,467	

Table 1. Design parameters for functionally graded lattice structures
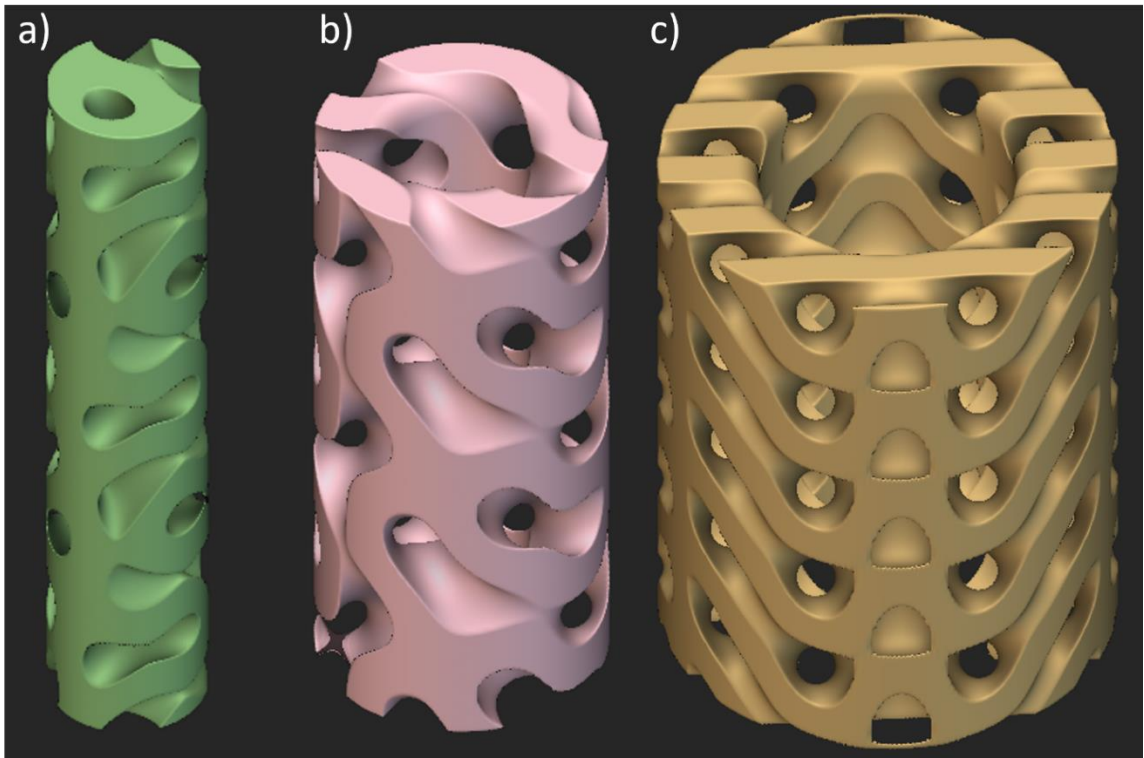
Figure 26. TPMS Lattice structures a) SplitP b) Gyroid c) Diamond
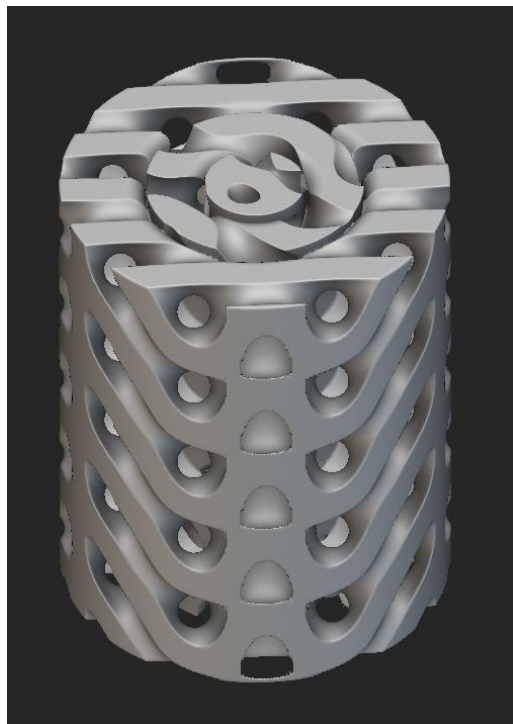
Figure 27. 1ˢᵗ sample
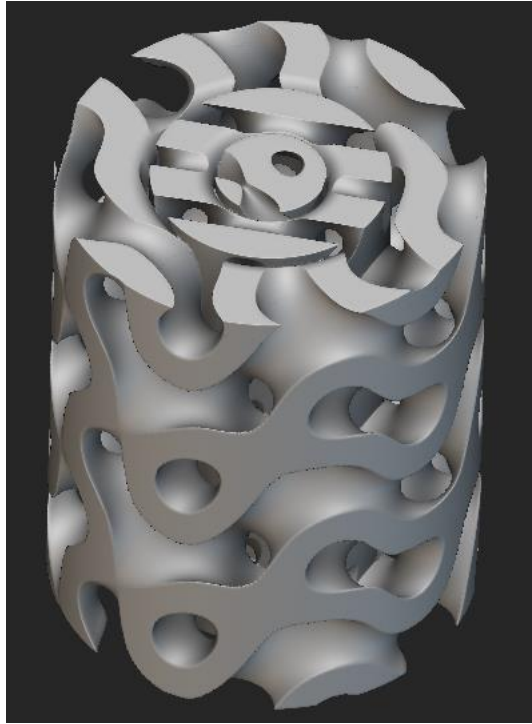
Figure 28. 2nd sample
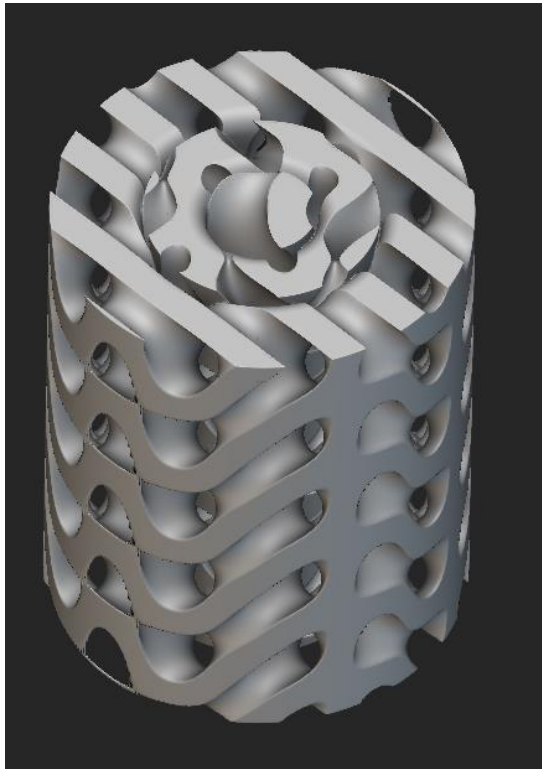
Figure 29. 3rd sample
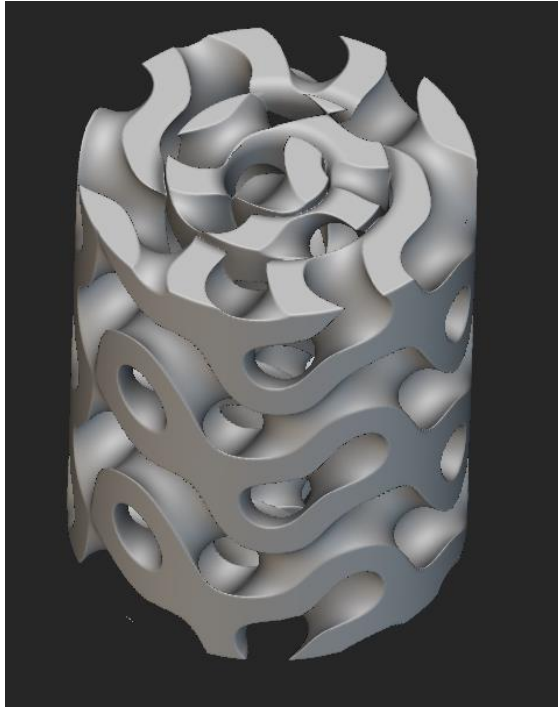
Figure 30. 4th sample
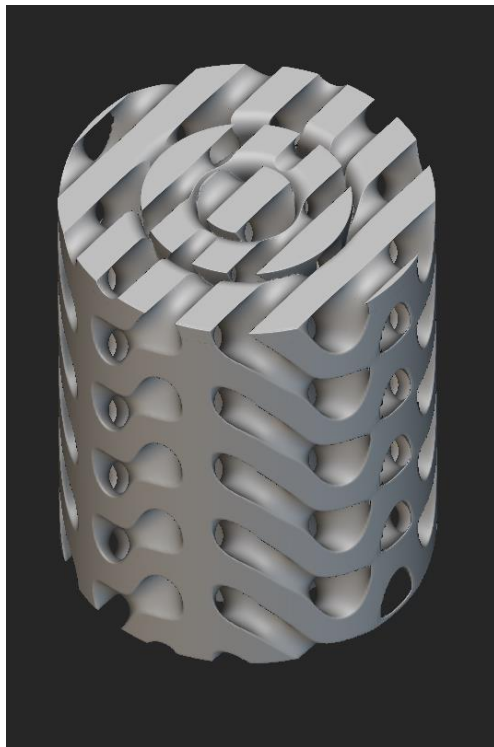
Figure 31. 5th sample
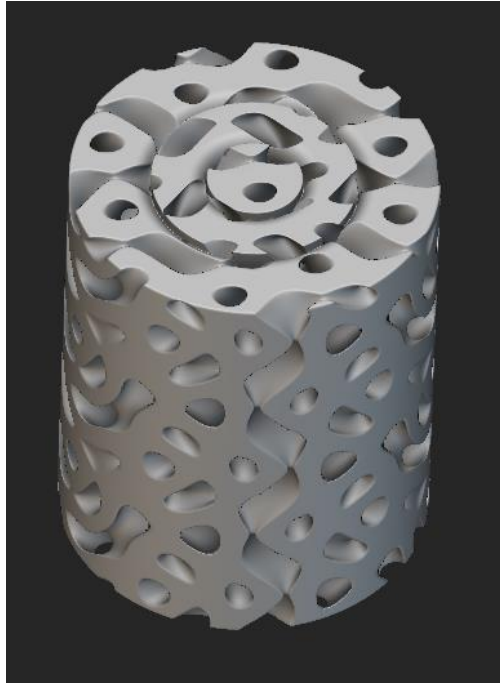
Figure 32. 6ᵗʰ sample
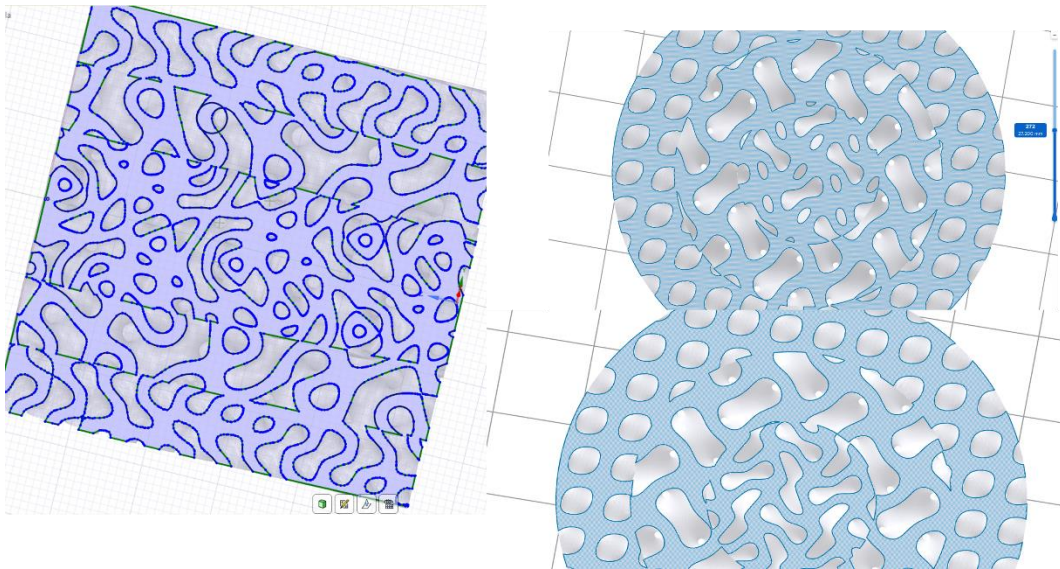
Figure 33. Cross section of cylinder and mergence between cylinders
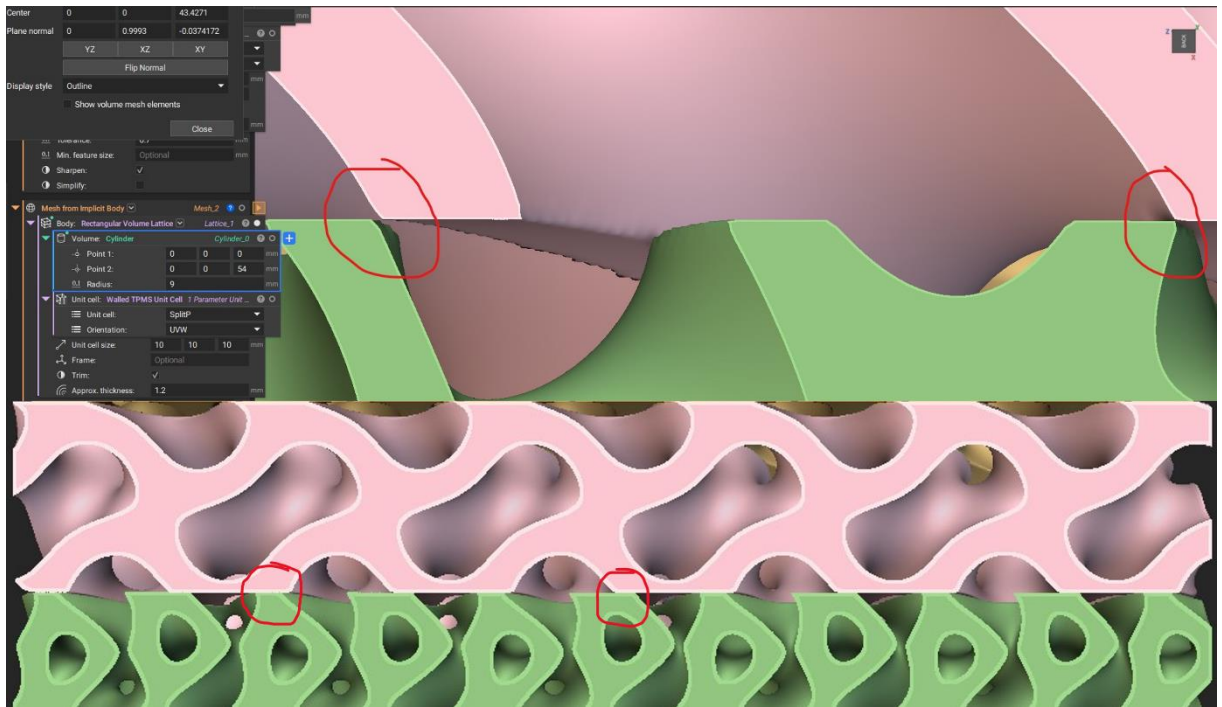
Figure 34. Before and after applying offset

4.2. Production and Material

The specimens were printed by using a Print Sharp M250 laser powder bed fusion (LPBF) machine. Print Sharp 250 is a medium volume machine for LPBF activities. Thanks to its flexible configuration with easily removable parts, a full powder change can be made in less than 2 hours [50]. Additionally, this system works with 0,5 kW Ytterbium (Yb) fiber laser, which focuses on the laser source to a spot size varying from 70 to 100 micrometers (µm).

The AlSi10Mg powder was used for printing. This material commonly used aluminum alloy due to its lightweight and good mechanical strength. To facilitate controlled ambient while printing process, the build volume was filled with argon gas at a flow rate of 7 liters per minute (l/min). This flow rate, in motion at a speed of 1.43 m/s. In addition, keeping oxygen level below 0.1% to avoid oxidation of the material was very important throughout the whole printing process.

Meanwhile, for minimizing residual stress and mitigate anisotropic behavior, a rotating scanning strategy was applied to the process. To avoid stress concentrations and symmetry along laser path, the commonly used angle setting 67 degrees was applied. In addition to facilitate the thermal conductivity and ensure good melting of powder during fusion, the build plate was preheated to 100℃. Therefore, this preheating phase prevented warping, and the quality of structure improved.

Figure 35. Print sharp 250 LPBF machine [50].

Building volume:	258x258x330
Build rate:	12-30cm^3/h (depending on material used and part geometry)
Deposition layer height:	0.02 – 0.1mm
Layer width:	0.1mm (single track width)
Laser power:	500W single mode IR fiber laser

Table 2. Technical data [50].

4.3. Surface Characterization

To observe the quality of printed samples, samples were cut in a cut-off machine at the laboratory of the DISAT department of the Politecnico di Torino. Afterwards, samples were polished to get rid of scratches from the cutting procedure. In this process, samples were polished with six different abrasive paper in rotating plate of polishing machine. Furthermore, images were taken from Optical Microscope (OM).
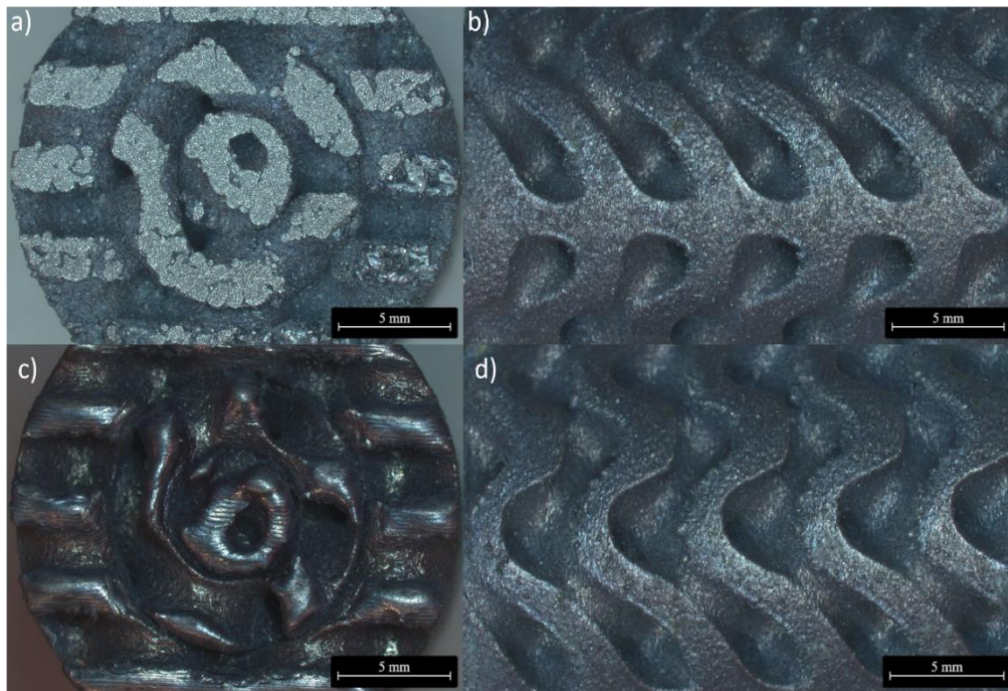
Figure 36. Cutting and Normal surface of the 1ˢᵗ sample

Figure 37. Cutting and Normal surface of the 2ⁿᵈ sample

Figure 38. Cutting and Normal surface of the 3ʳᵈ sample

Figure 39. Cutting and Normal surface of the 4ᵗʰ sample

Figure 40. Cutting and Normal surface of the 5th sample
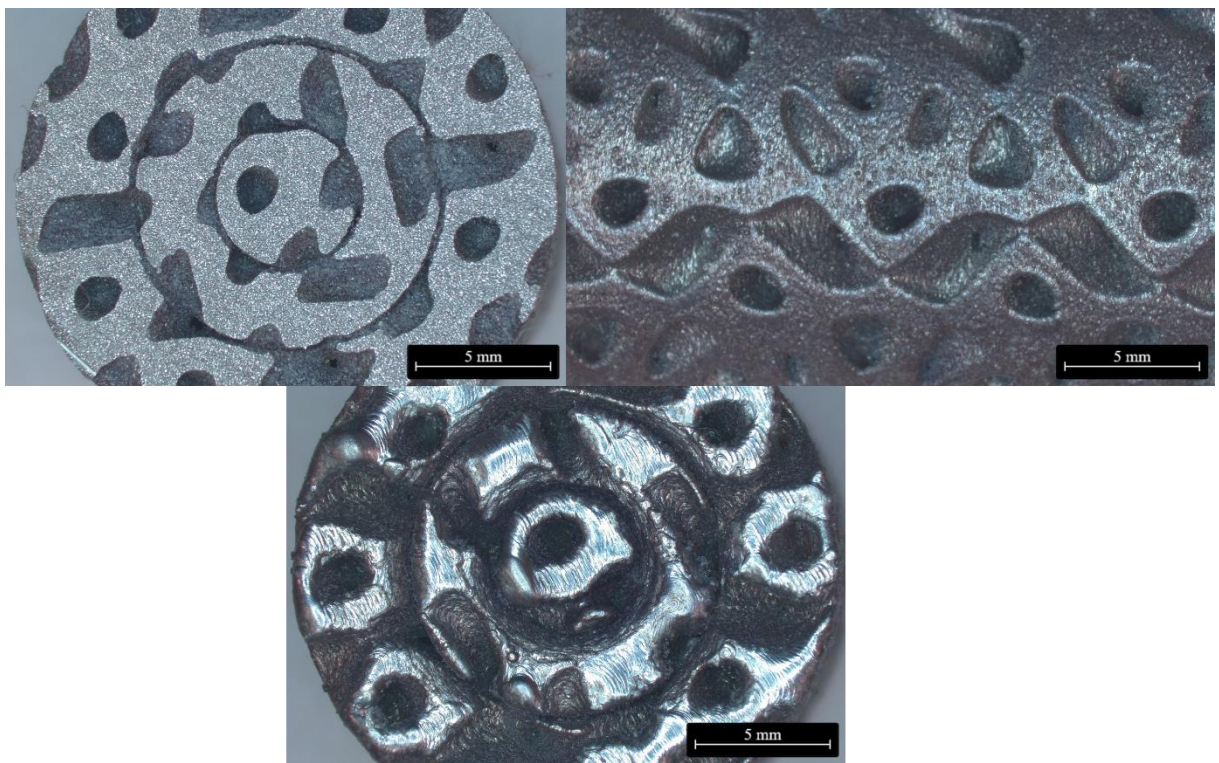
Figure 41. Cutting and Normal surface of the 6th sample

35

As can be seen in the pictures almost all TPMS structure types were intact. However, when we look from top and cut the surface of 3rd sample, there is a small droplet shape void. This phenomenon can be attributed to the relationship between melting pool and process parameters. In literature, it has been stated that disrupted movements of melt pool can affect porosity, and improper wetting can trigger balling effect (spherical droplets). This instability is called Plateau-Rayleigh instability [37-38]. Therefore, this event can cause variation in thickness of next powder layer then cause binding defect between layers [37].

4.4. Mechanical Performance

Uniaxial compression tests were performed. Samples were placed between two plates. While the upper one was moving with a constant strain which was 2 mm/min up to the densification of the pressed lattice structure, bottom plate was fixed. Uniaxial loading was applied parallel to the building direction along the z axis.

5. RESULTS AND DISCUSSION

5.1. Compression Test

From the experimental test result in laboratory, stress-strain curves were extracted. From the Force (Newton) and displacement (mm) values.

$$\sigma = \frac{F}{A}$$
$$\varepsilon = \frac{\Delta l}{l_0}$$

Basically, all samples had similar stress-strain behaviors so that they can be divided into 4 stages: the first stage is the linear elastic region, and the second one is elastic-plastic stage which has yield point. Then third is yield plateau and the last is densification stage.

From the 1st to 6th sample there was a certain elastic region until yield points and then stress increased rapidly with a linear behavior just like in Hook's law. Afterwards, curve elastic-plastic stage starts.

The elastic-plastic stage has a long increasing part after the elastic region and then stress will decrease after reaching yield point. This phenomenon is called the strain softening process. Afterwards densification starts and continuously increases [42]. This is due to the surfaces piling and encountering each other and causes an increase in the stress. Finally, all samples had stretch-dominated behavior and as mentioned in the literature, this is advantageous for a lightweight design [40].
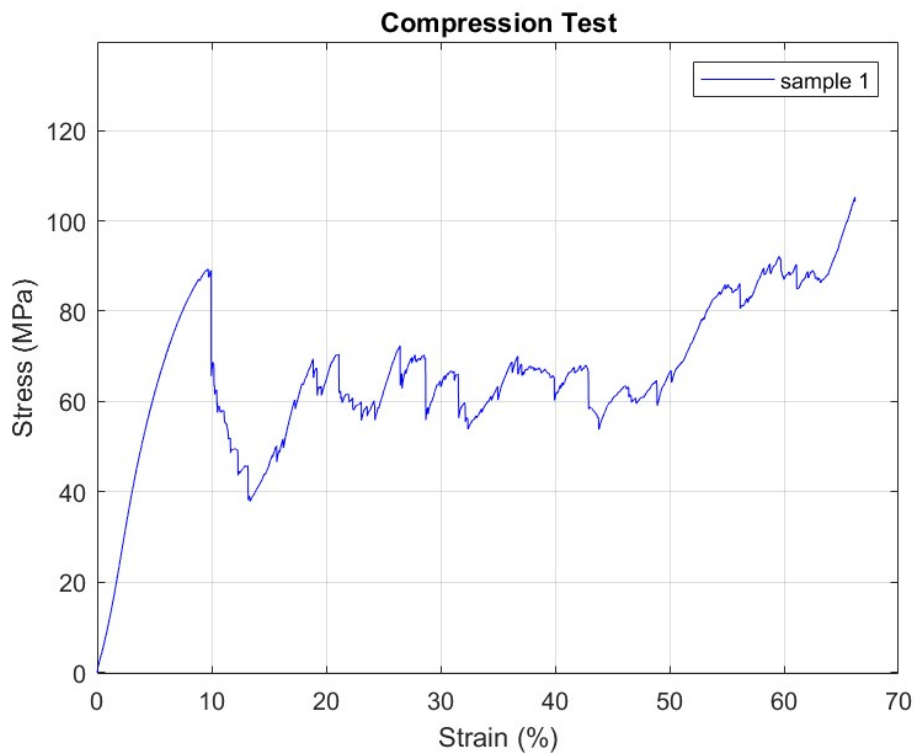
Figure 42. Stress-strain diag. of 1st sample
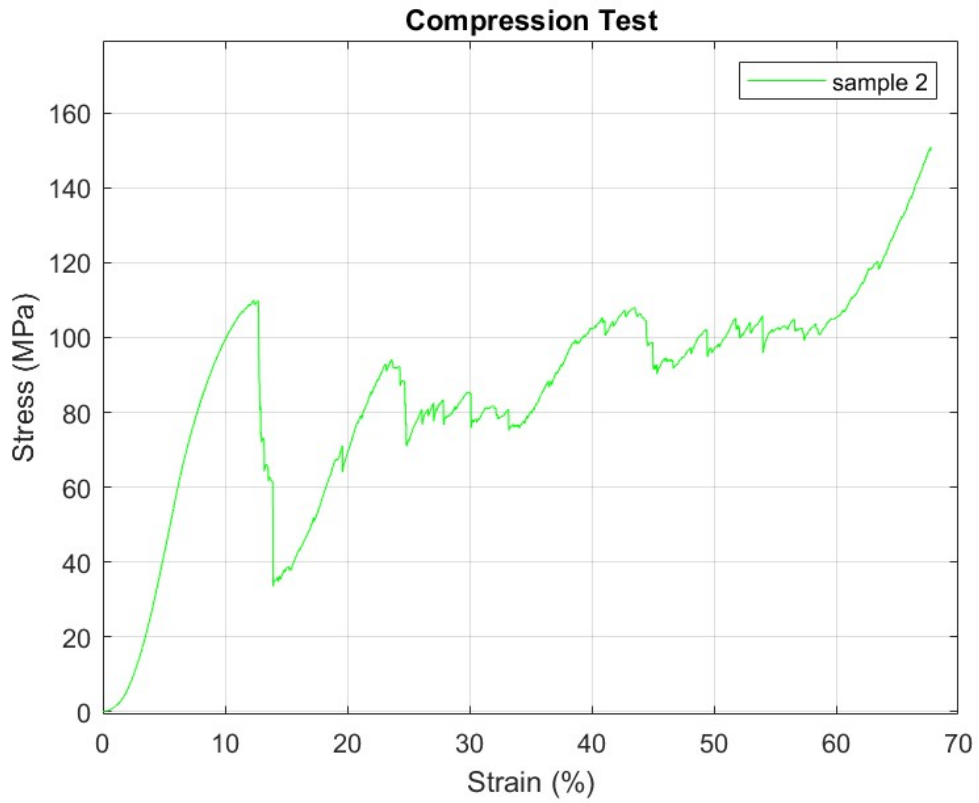
Figure 43. Stress-strain diag. of 2nd sample
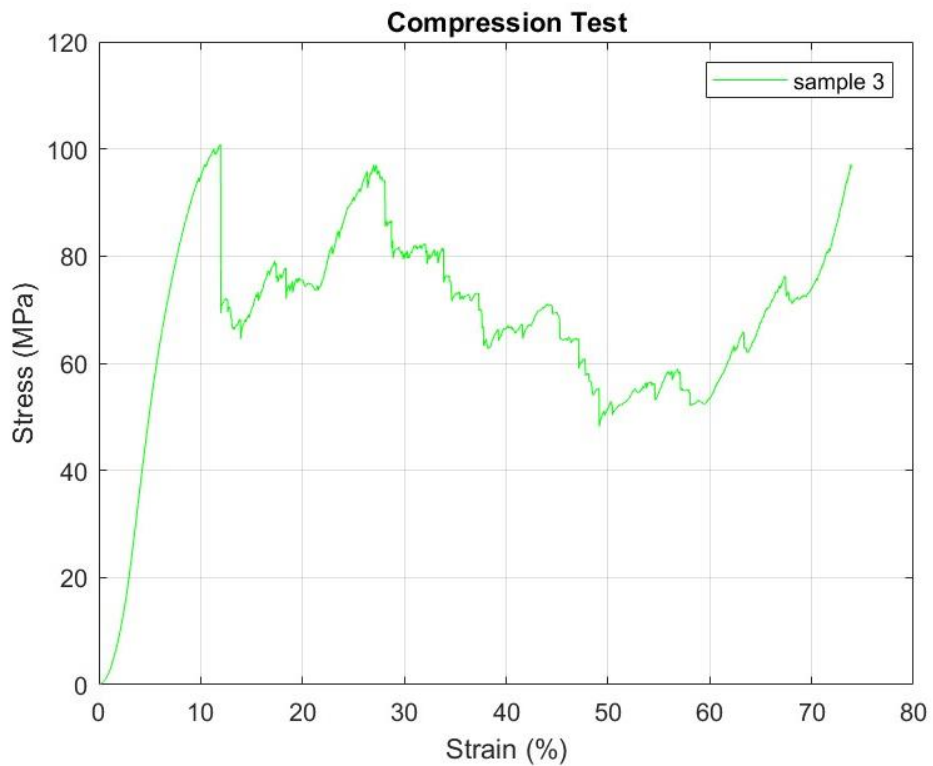
Figure 44. Stress-strain diag. of 3rd sample
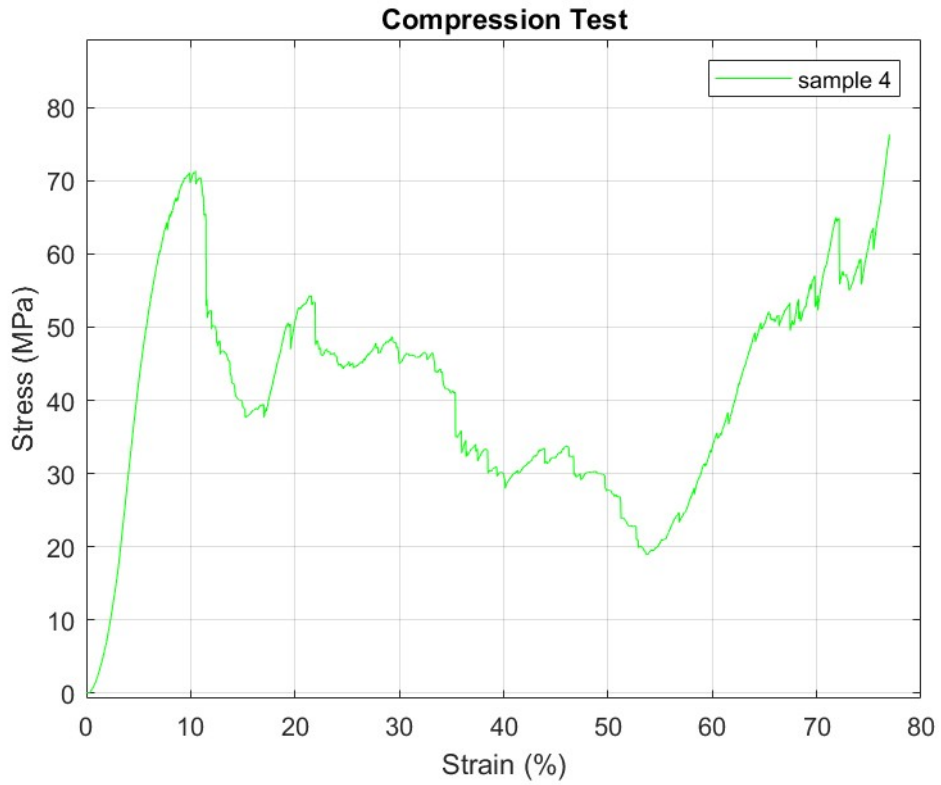
Figure 45. Stress-strain diag. of 4th sample
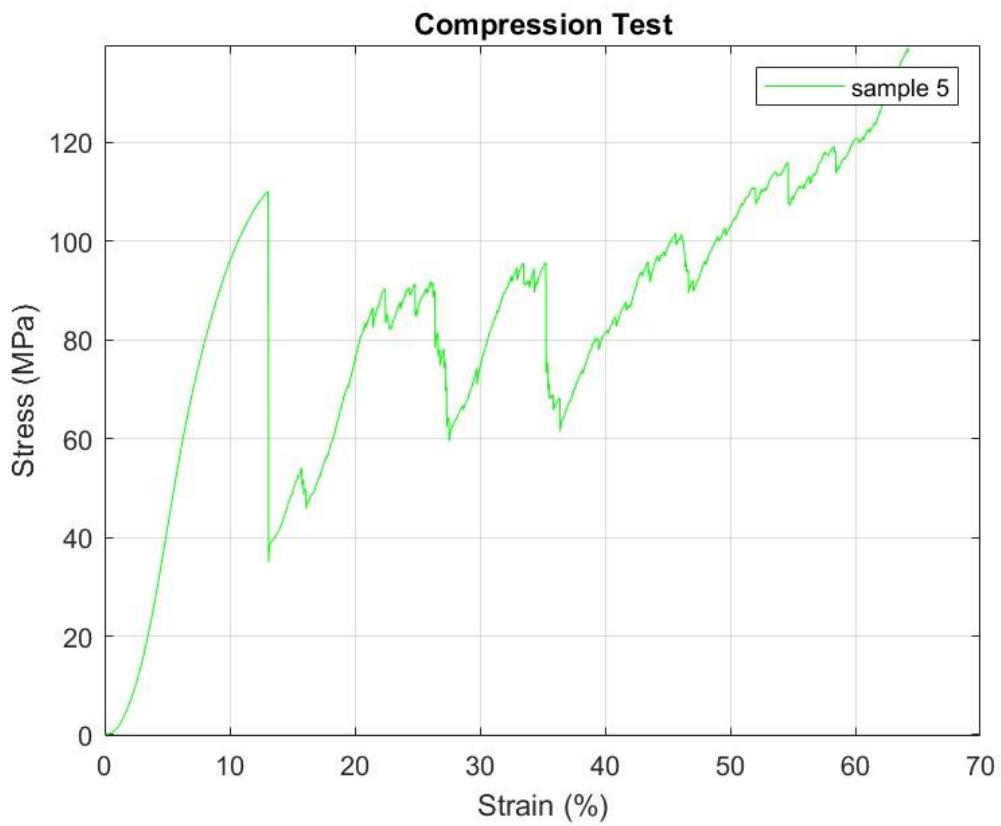
Figure 46. Stress-strain diag. of 5th sample
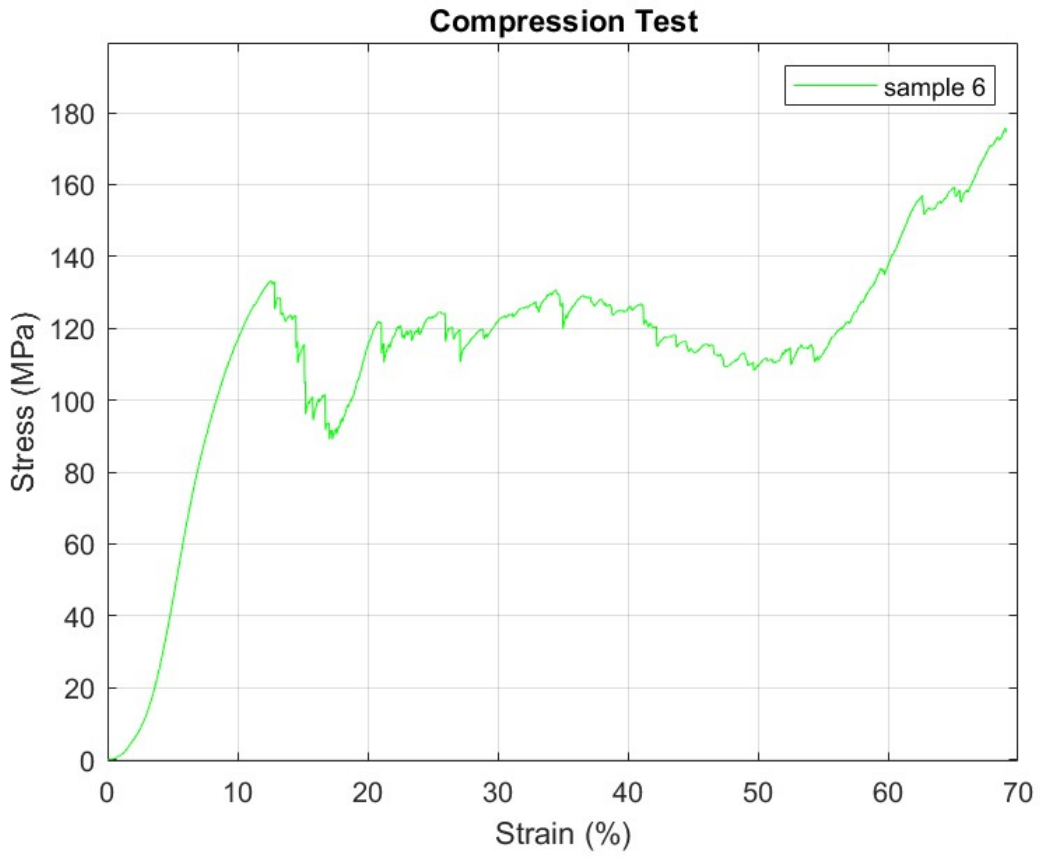
Figure 47. Stress-strain diag. of 6th sample
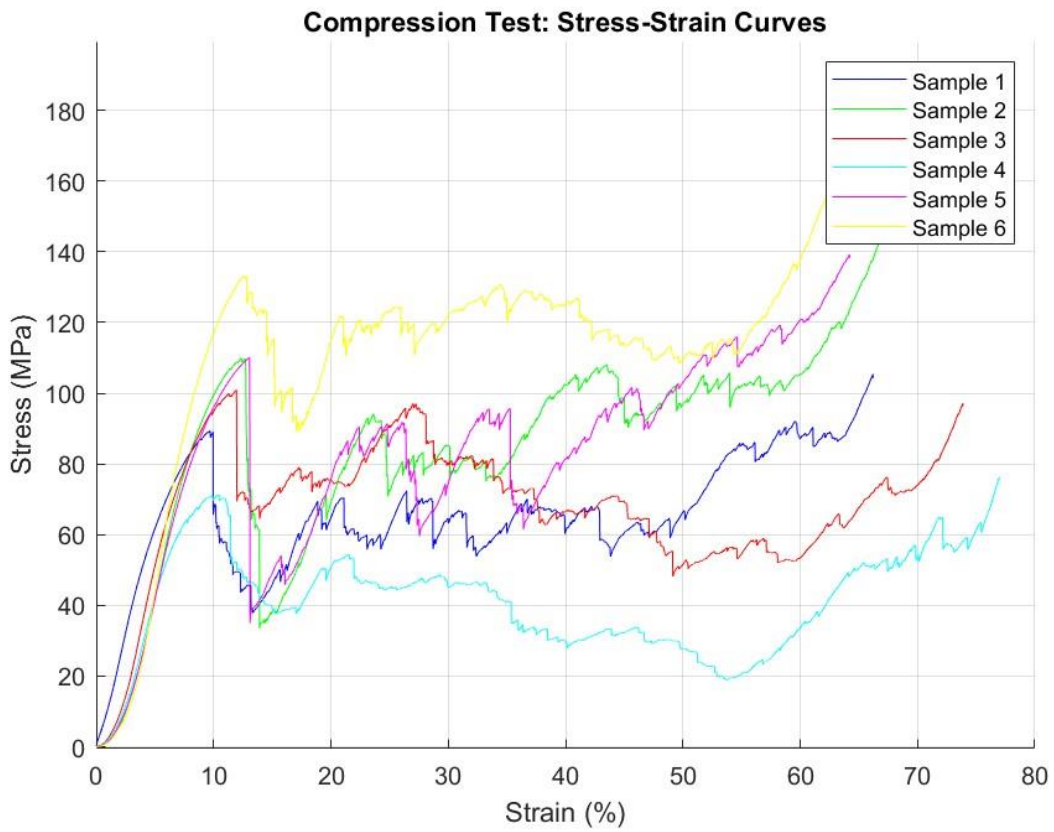
Figure 48. Stress-strain diag. of all samples

40

	UCS (ultimate compressive stress MPa)	UCStrain (ultimate compressive strain %)	E (Young Modulus MPa)	Yield Strength (MPa)
1st sample	105.28	66.18	118.73	89.39
2nd sample	150.85	67.72	216.58	110.03
3rd sample	100.83	67.70	99.45	89.39
4th sample	76.27	76.96	56.89	71.32
5th sample	139.26	64.21	152.08	110.10
6th sample	175.79	69.01	205.70	133.24

Table 2 Results of compression test

When we analyze the results of compression test, FGL models with varying lattice in type along the model have similar results with uniform lattice structures. However, when we compare UCS values of specimens' 6th sample is superior to other samples. When we look at UCStrain values, the first three samples have similar failure behavior.

5.1.1. Young Modulus

By evaluating all stress-strain curve from data, it was possible to derive the Young´s Modulus as an index of the stiffness of the specimens. As mentioned in literature, Young´s Modulus can be derived from linear elastic region. Basically, taking slope of the linear line defined between two different stress limits. When all results considered, stiffness of samples are in line with the UCS results. For example, even though slightly lower in UCS 2nd sample (Split P, Diamond Gyroid) higher young modulus than the rest. Additionally, 6th sample (fully Split P) has the second highest stiffness value. Another interesting result was 5th sample (fully Gyroid) has good UCS and young modulus values among others.
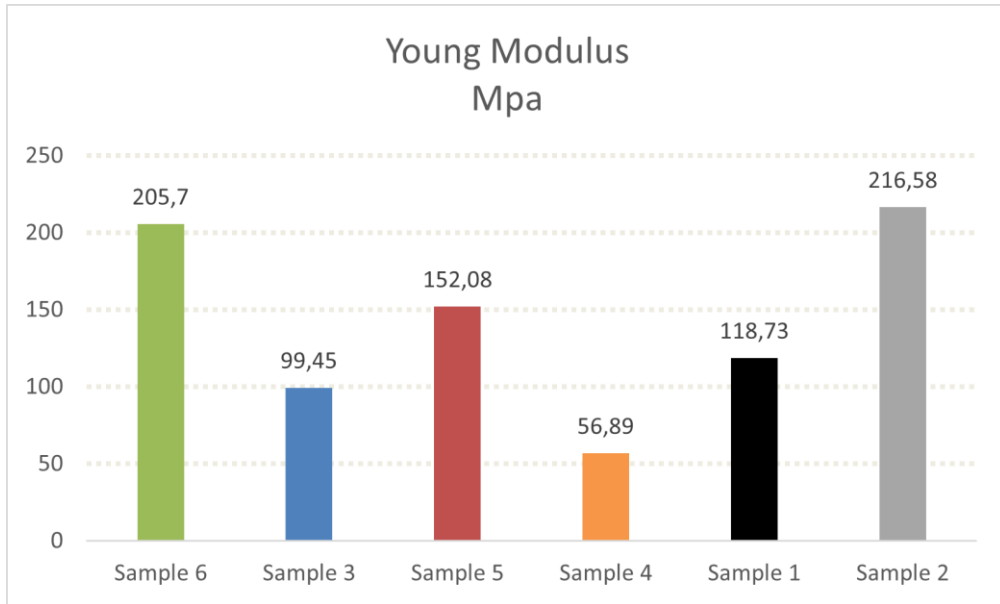
Figure 49. Young modulus diag. of samples

5.1.2. Yield Strength

The yield strength of specimens corresponds to the point where material begins to deform plastically. This value, often referred to to determine the maximum allowable load in stress calculations. The values that were taken from Stress-Strain curves show that yield values are parallel to the UCS and Young modulus results.
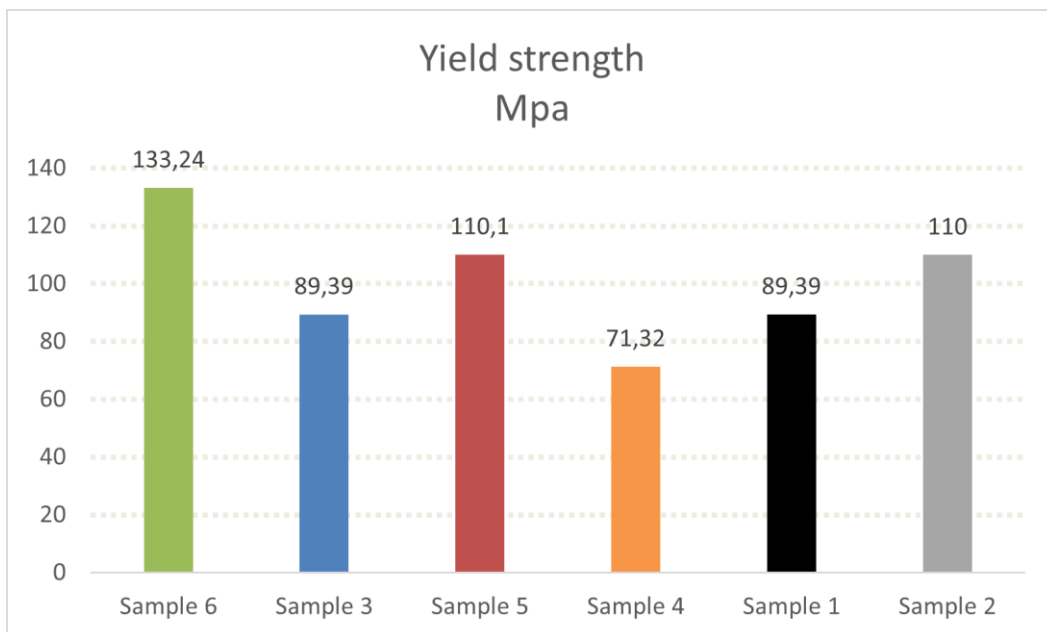
Figure 50. Yield strength diag. of samples

42

5.1.3. Specific Energy Absorption

As it has been stated in the literature the area under the elastic region of Stress-Strain curve can give the toughness capacities of the materials [39]. Basically, energy absorbance until failure. However, in this study the sample did not fail so that beginning of densification stage was taken as limiting point [40].

Therefore, the specific energy absorption (SEA) is calculated as:

where:

σ is the stress (in MPa or N/mm²),

ϵ is the strain

$$\text{SEA(J/g)} = \frac{EA}{M} = \frac{\int_0^\delta F \, d\delta}{M} = \frac{\int_0^\epsilon \sigma(\epsilon) \, d\epsilon}{\rho *}$$

Where M is the mass of the lattice structure, F is the force, AE is the total energy absorbed by the material, which can be calculated by the area under the load-displacement curves. Generally, a higher toughness represents a better energy absorption capacity of the cellular material [24]. As can be seen in the figure above, sample-3 which is composed with diamond from outer diameter and integrated SplitP sample-6 has better energy absorption capacity than other samples.
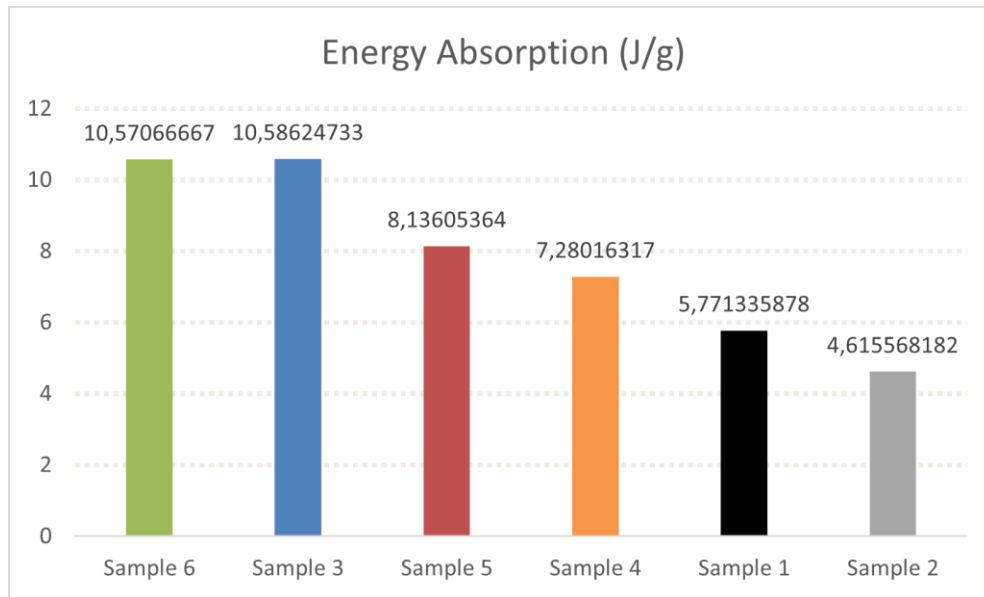
Figure 51. Specific Energy Absorption diag. of samples

5.2   Simulation Analysis

As mentioned in numerical simulation theory section, simulation is a key for predicting the behavior of lattice structures. In this study, homogenization was applied to compare different types of lattice structures with the same unit cell. The homogenization was applied using nTopology software, to evaluate the mechanical and displacement behavior of the lattice structure. This method allows to obtain stiffness matrix for a given geometry. Inside of nTopology there is a feature which runs the entire simulation. By starting from implicit body to surface mesh then remeshing stage for quadratic solid mesh was performed.

Afterwards, to define homogenize unit cell, Fe solid model and volume mesh defined by setting specific edge length with minimum feature size values. Finally, to run the homogenization material which AlSi10Mg was defined. In addition, software sets boundary conditions and forces. The six forces (3 axials, 3 shears) are applied. As a result, it was possible to get the displacement in a specific direction (in this case Z coordinate due to compression) and directional stiffness. This directional stiffness allows us an idea of how geometry behave according to different coordinates.

The following figures explain:

- The images of mesh that applied

44

- The image of displacement (mm) in the Z-direction
- The directional stiffness with the young modulus
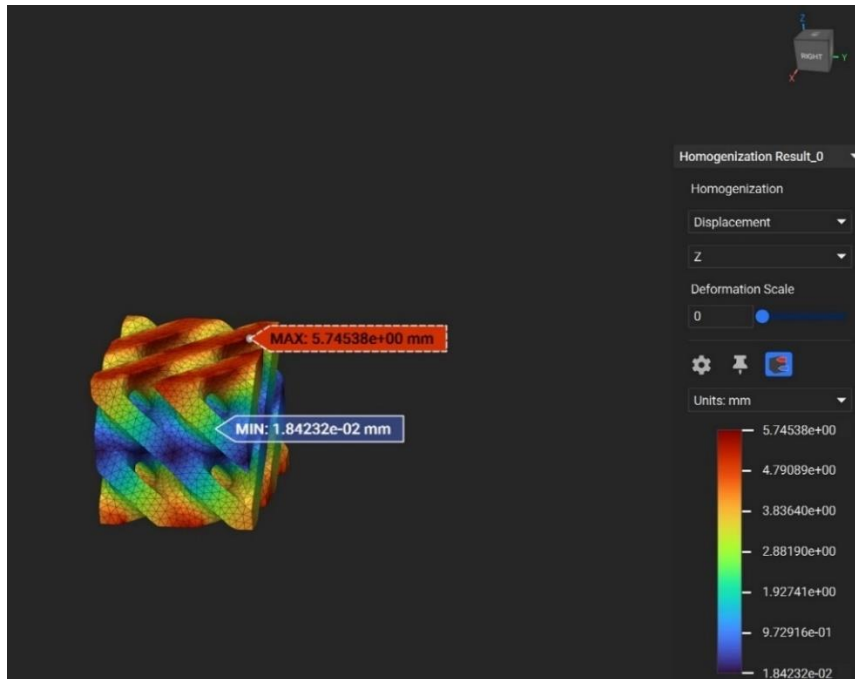
Figure 52. Displacement of Diamond cell
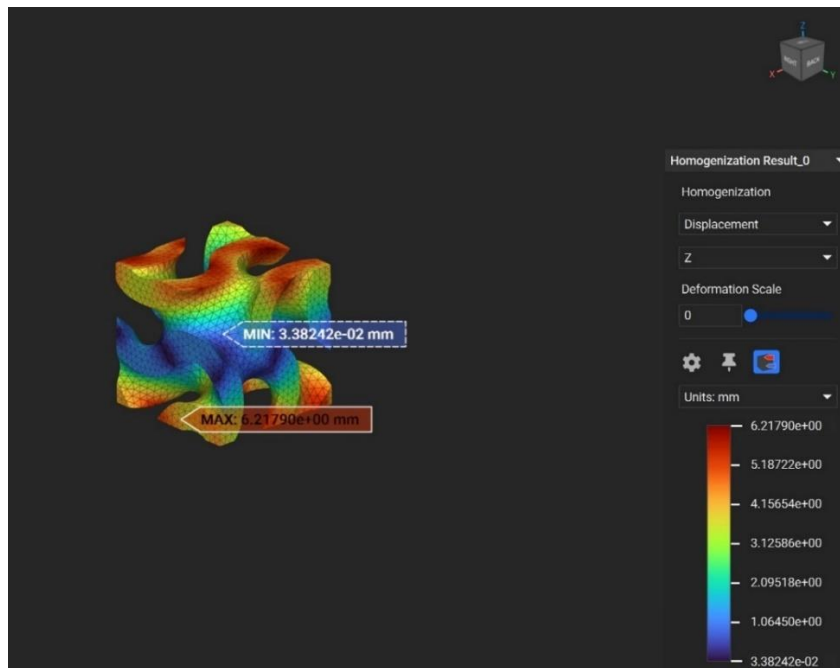
Figure 53. Displacement of Gyroid cell
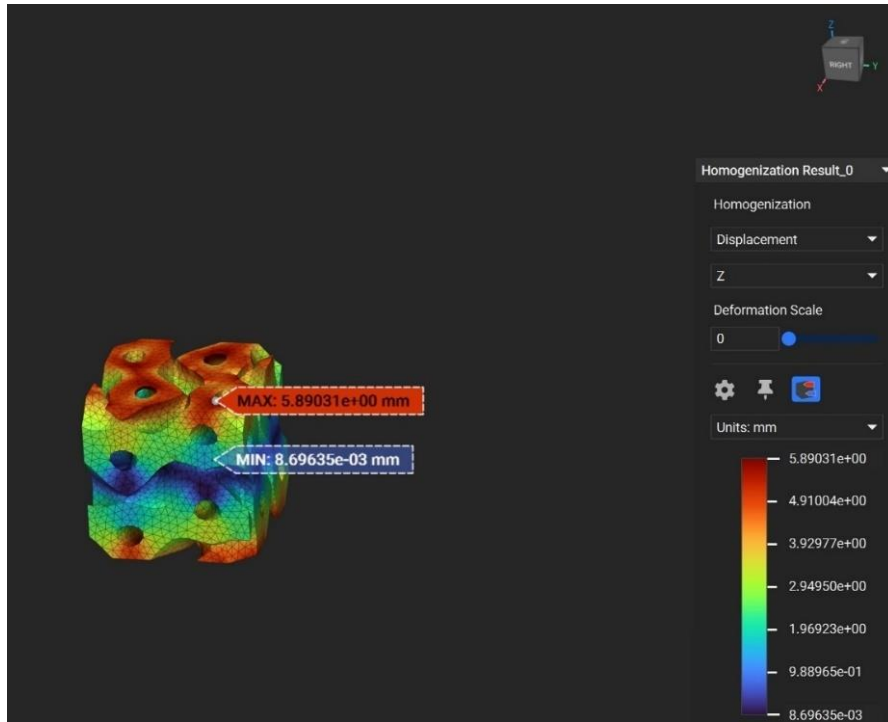
Figure 54. Displacement of Splitp cell
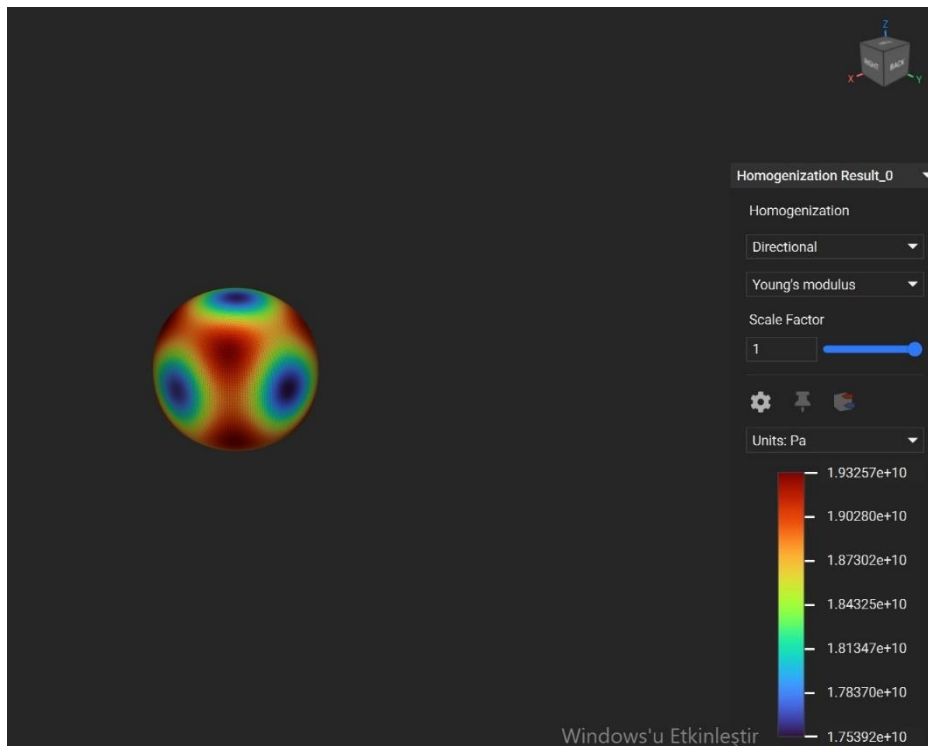
Figure 55. Young modulus of Gyroid
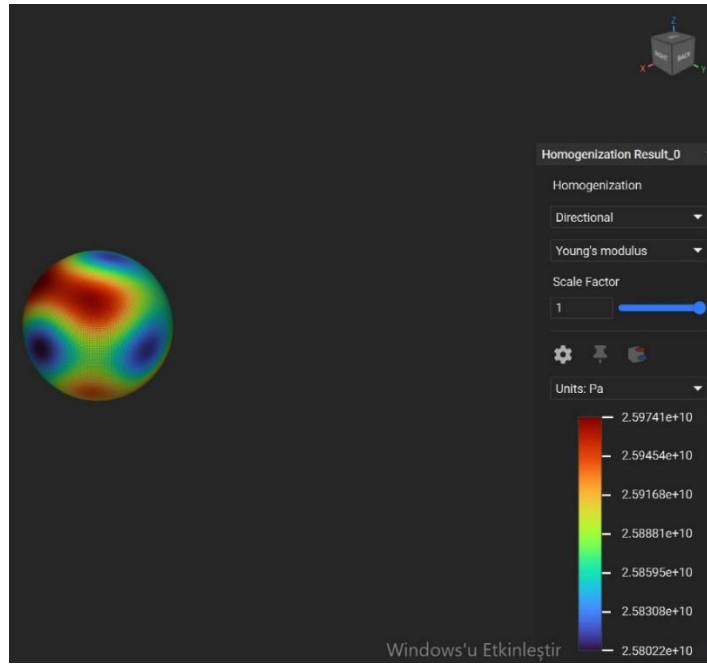
Figure 56. Young modulus of Diamond
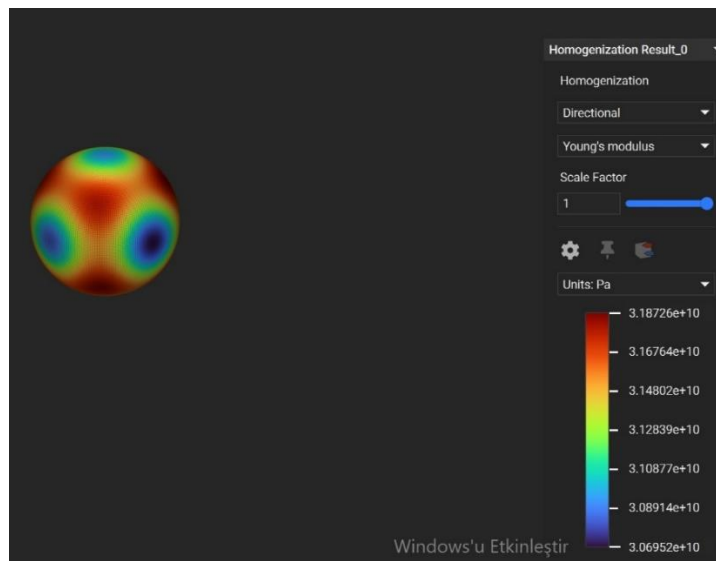
Figure 57. Young modulus of SplitP

TPMS homogenized structures	Displacement (mm)	Young Modulus (GPa)
Diamond	5,74	25,97
Gyroid	6,21	19,32
SplitP	5,89	31,87

Table 3. Homogenization simulation analysis

Finally, when displacement along Z-directions is considered, Diamond and SplitP TPMS structures had lower deformation than gyroid. Another result was, SplitP homogenized TPMS structure had superior young modulus than other structures. This result is also proportional to compression test results.

5.3. Deformation Mode

The deformed structures are illustrated below in Fig. presenting the FGL's from 1st to the 6th sample respectively. All the lattice structures exhibit similar behavior in elastic regions where the displacement increases proportionally. As stress increases, the strain rate also increases. Consequently, all lattice structures reach the highest point in terms of an applied load, after which the stress decreases dramatically. As explained above all samples were stretch dominated and they undergone buckling and collapses. In literature, the same event occurred on beam-based structures which were stretch-dominated [34].

In another research, stretch-dominated lattice structures presented the same stress-strain behavior as in this study. Additionally, they had strain softening due to buckling of struts [42].
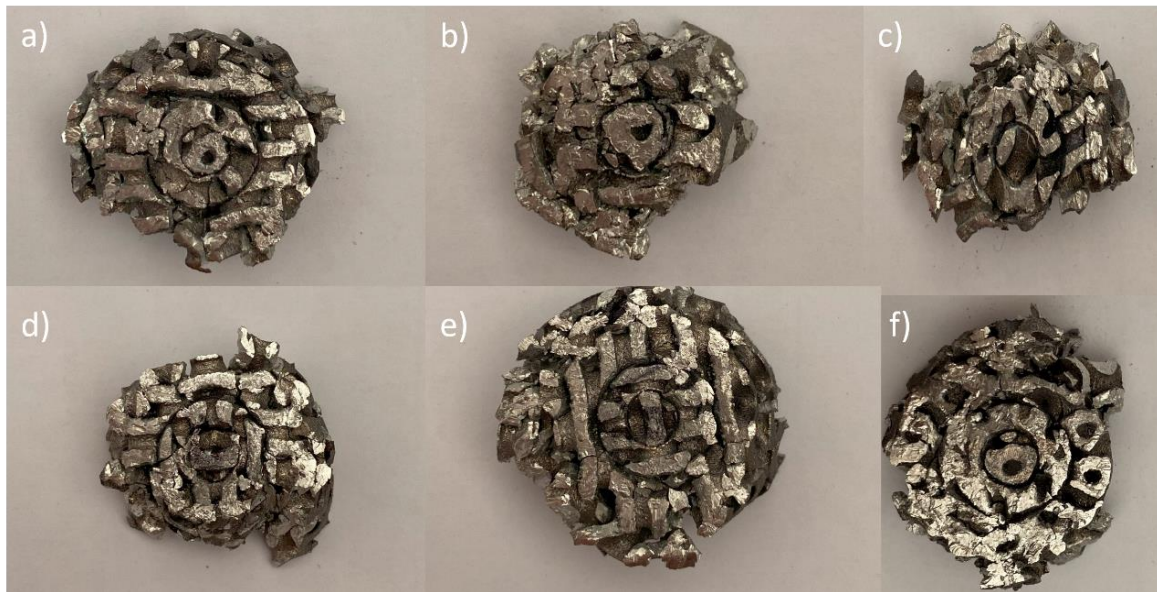
Figure 58. Deformation modes of all samples
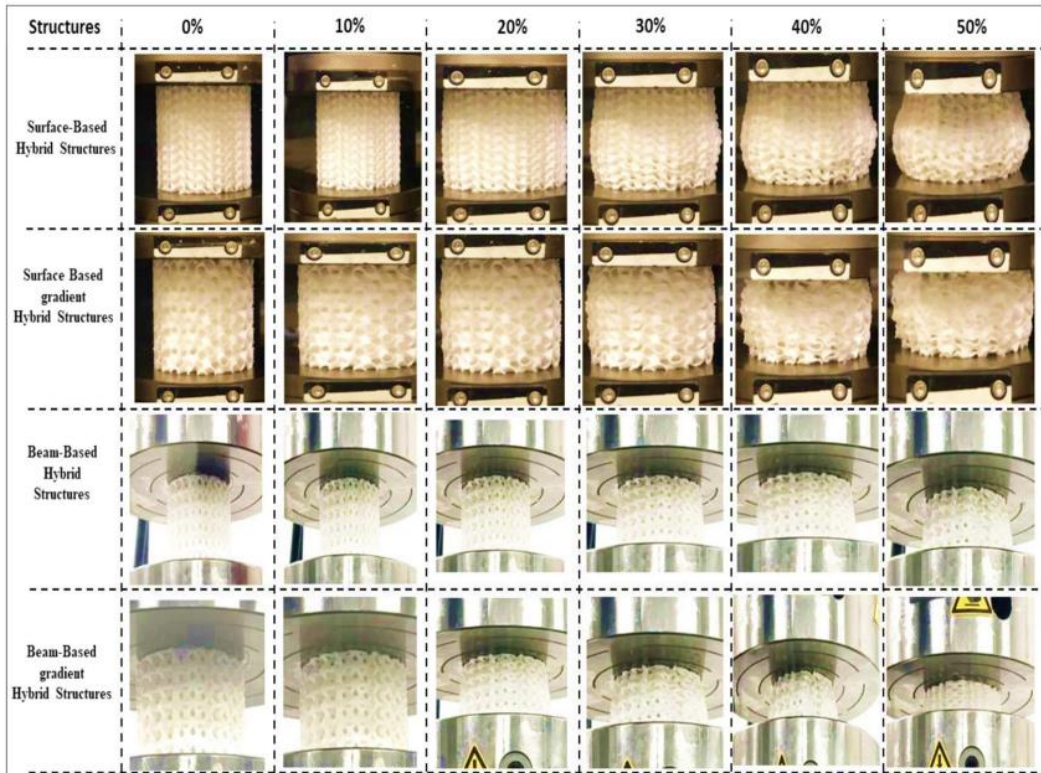
Figure 59. Deformation mode of samples in another research [34].

$\varepsilon = 1\%$ $\varepsilon = 10\%$ $\varepsilon = 20\%$ $\varepsilon = 30\%$ $\varepsilon = 40\%$

(a)

$\varepsilon = 1\%$ $\varepsilon = 10\%$ $\varepsilon = 20\%$ $\varepsilon = 30\%$ $\varepsilon = 40\%$

(b)

$\varepsilon = 1\%$ $\varepsilon = 10\%$ $\varepsilon = 20\%$ $\varepsilon = 30\%$ $\varepsilon = 40\%$

(c)

$\varepsilon = 1\%$ $\varepsilon = 10\%$ $\varepsilon = 20\%$ $\varepsilon = 30\%$ $\varepsilon = 40\%$
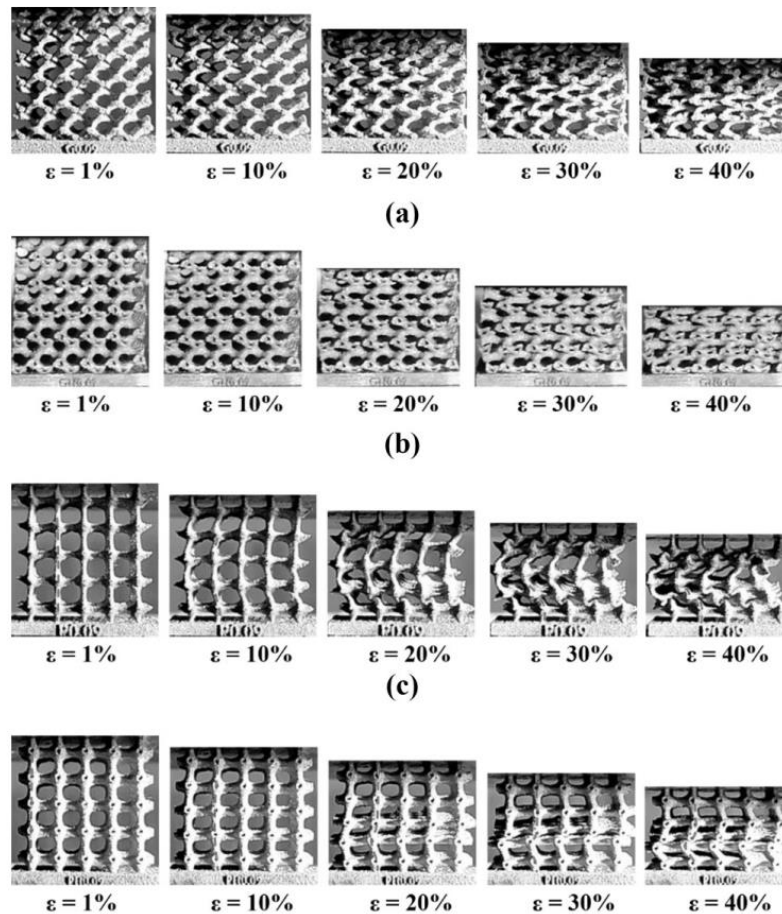
Figure 60. Strain softening and buckling of struts in the literature [42].

49

5.4. Metallography Images

When all metallography images were investigated from OM, there were small voids and cracks in microscale in between transition layers. This can be attributed to the off-set settings during design procedure in the nTopology software. Because to create union there had to be applied some off-set values to fill gaps as in <mark>Fig.</mark> below.

However, this delamination weren´t monitored during observation of transition layers. Another reason also can be attributed to the approximate thickness values between these regions.
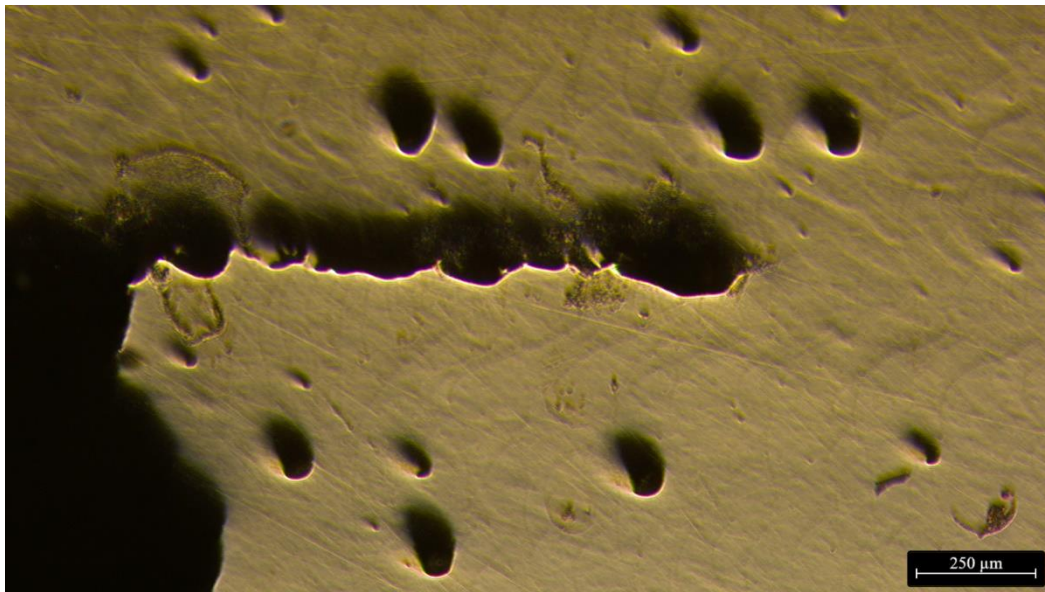
Figure 61. OM image of 1st sample
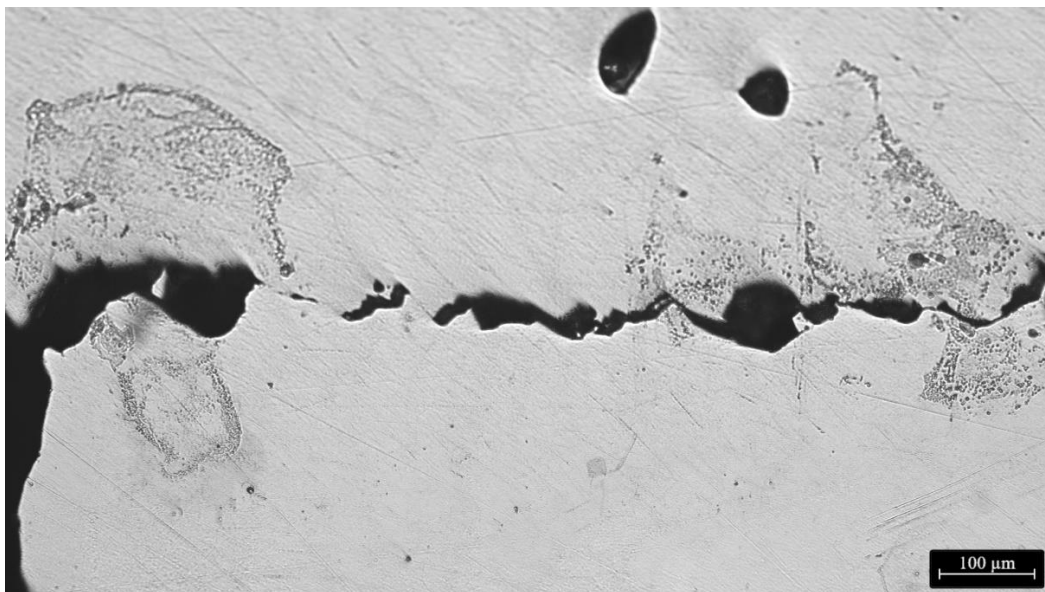
Figure 62. OM image of 1st sample
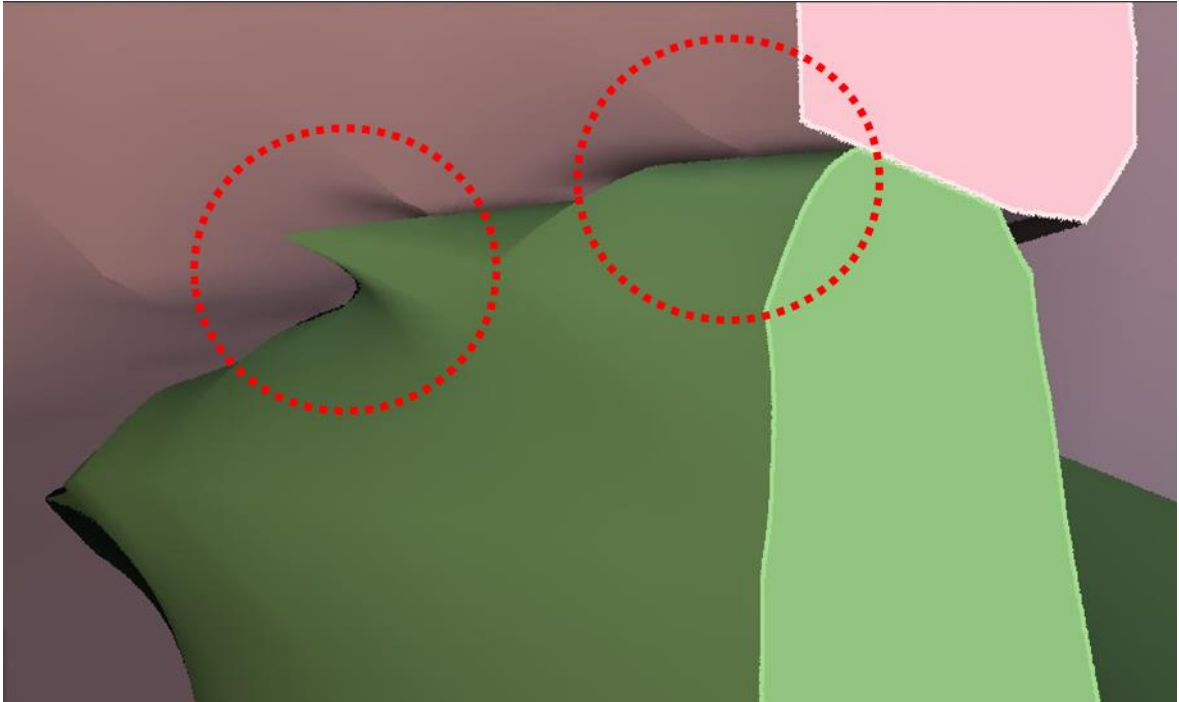
Figure 63. Transition layer without off-set
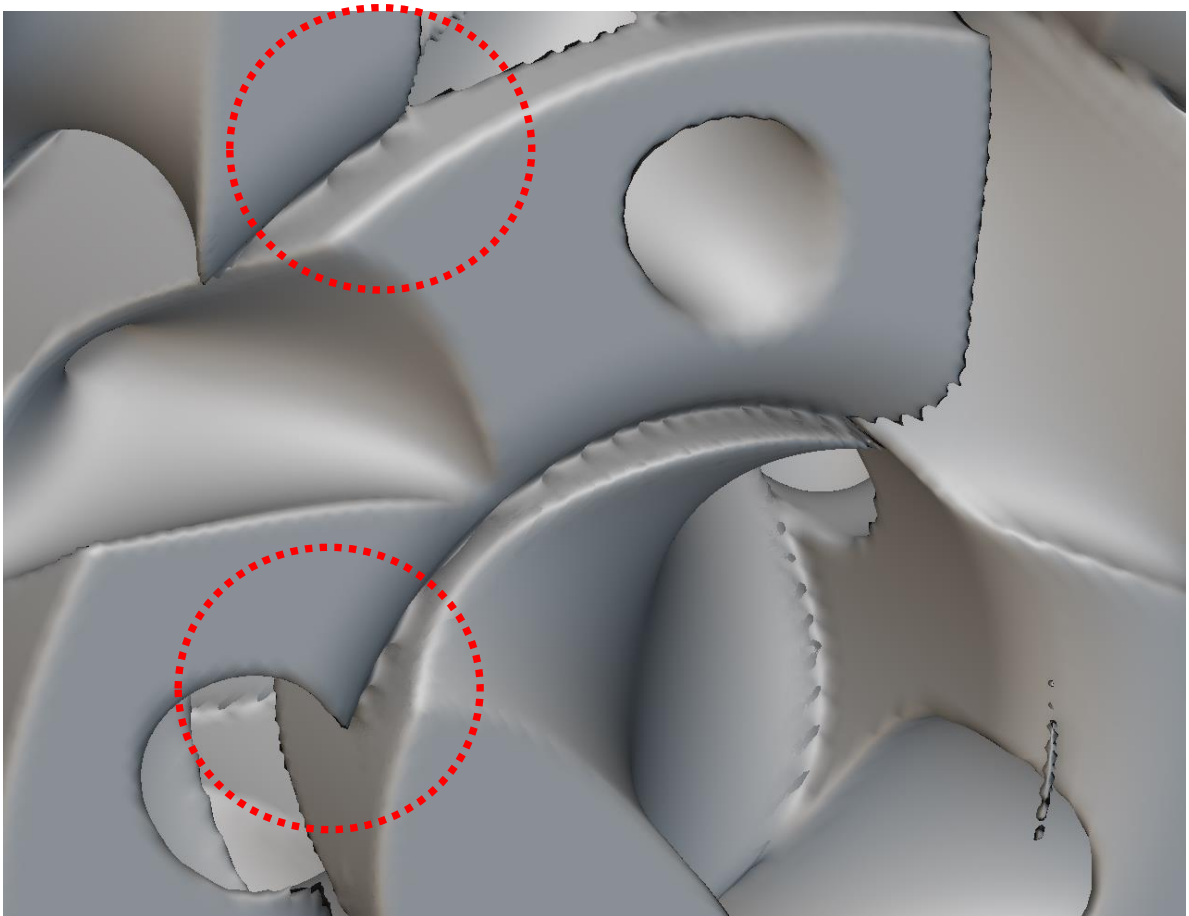
Figure 64.Transition layer without off-set

6.   CONCLUSION

In this study by varying relative density and unit cell size of TPMS samples were designed to imitate cancellous bone of human body. In the experimental part, samples were printed and their mechanical, energy absorption and surface characteristics were evaluated. The aim of this study was to contribute to structural applications of functionally graded lattice structures.

All in all, when all results are considered summary of this work can be listed as follows:

- All TPMS FGL structured had stretch-dominated behavior and undergone strain softening during compression test. According to literature review, AlSi10Mg stretch-dominated samples can be applied in load carrying purposed designs,

- In terms of compressive strength, energy absorption and young modulus there wasn´t any strict difference in between composed and one unit cell designs,

- 6th sample which is designed from one-unit SplitP cell had superior ultimate compressive strength, young modulus and specific energy absorption.

- The 2nd sample, which was composed of 3 different TPMS cells (SplitP, Diamond and Gyroid) had the second best mechanical and specific energy performance after the 6th sample.

- When homogenization numerical analysis and experimental results are compared SplitP had superiority in terms of mechanical properties.

- All samples had the same deformation mode and undergone buckling phenomena.

- OM pictures show that macroscale transition of layers was smooth and without defects. However, in microscale it was evident that there were cracks and delamination,

For the future, the study can be improved regarding process and design parameters. Therefore, the difference between design and production stages can be reduced to minimum.

7. APPENDIX
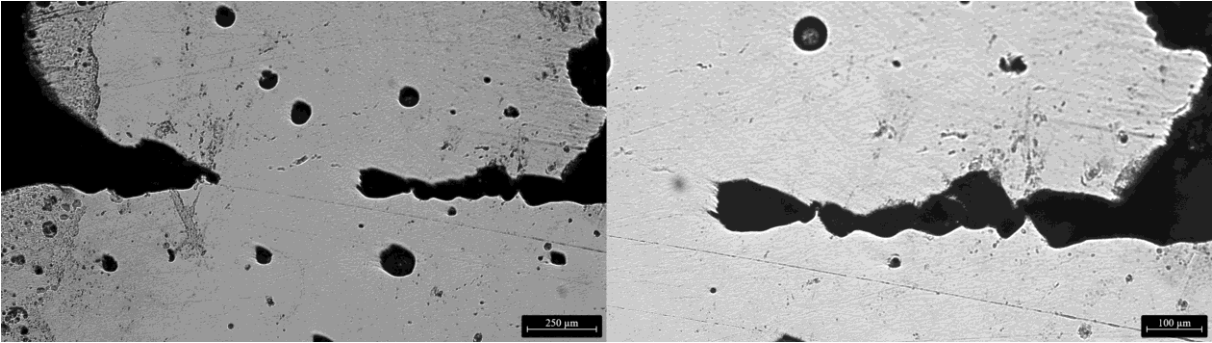
Figure 65. OM image of 2nd sample
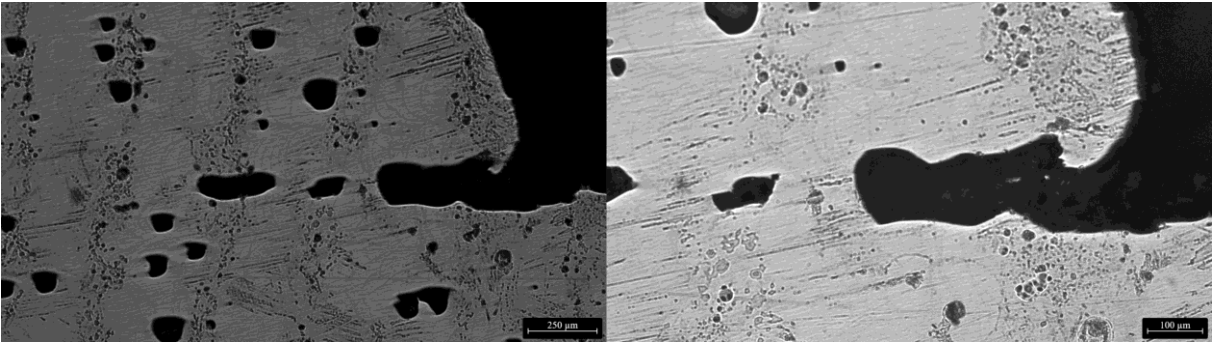
Figure 66.OM image of 3rd sample
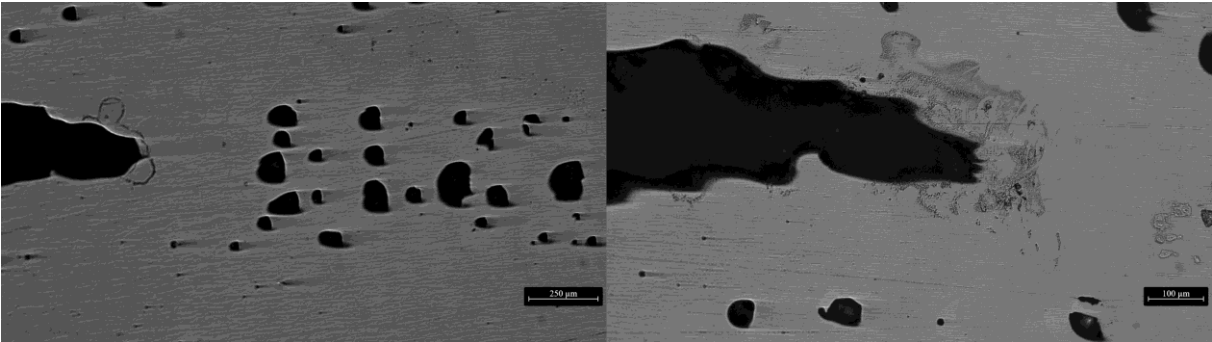
Figure 67. OM image of 4th sample
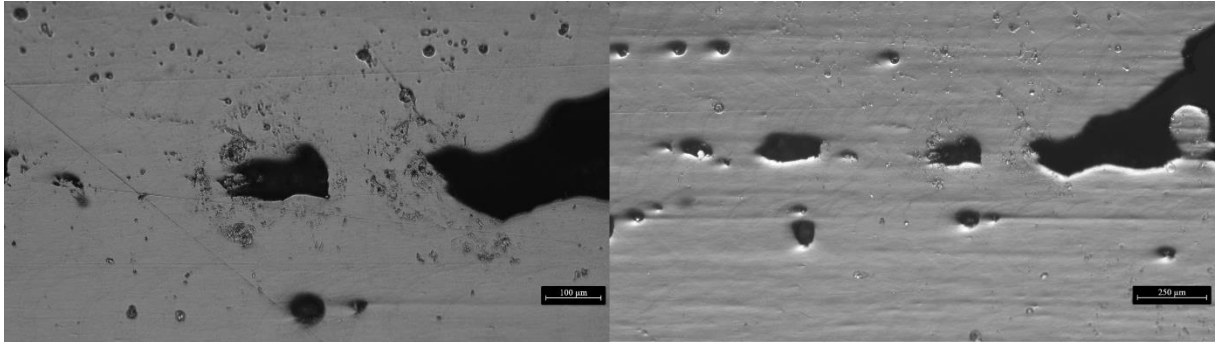
Figure 68.OM image of 5th sample
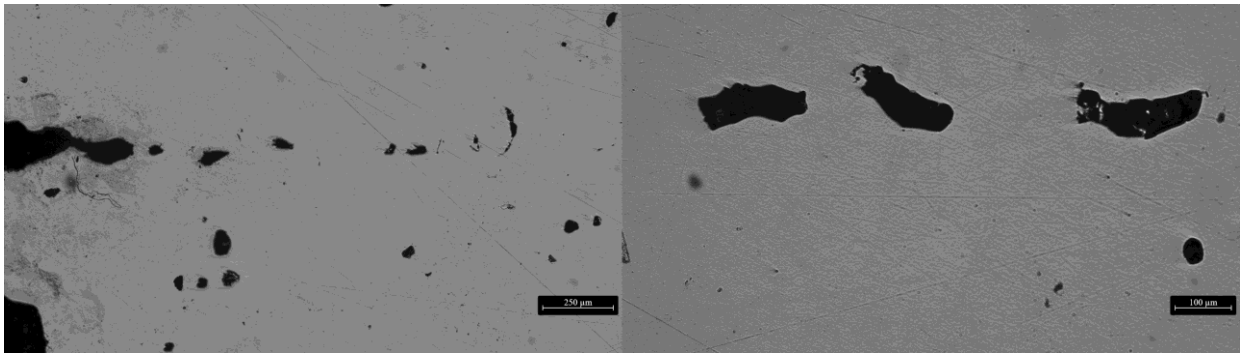
Figure 69. OM image of 6th sample
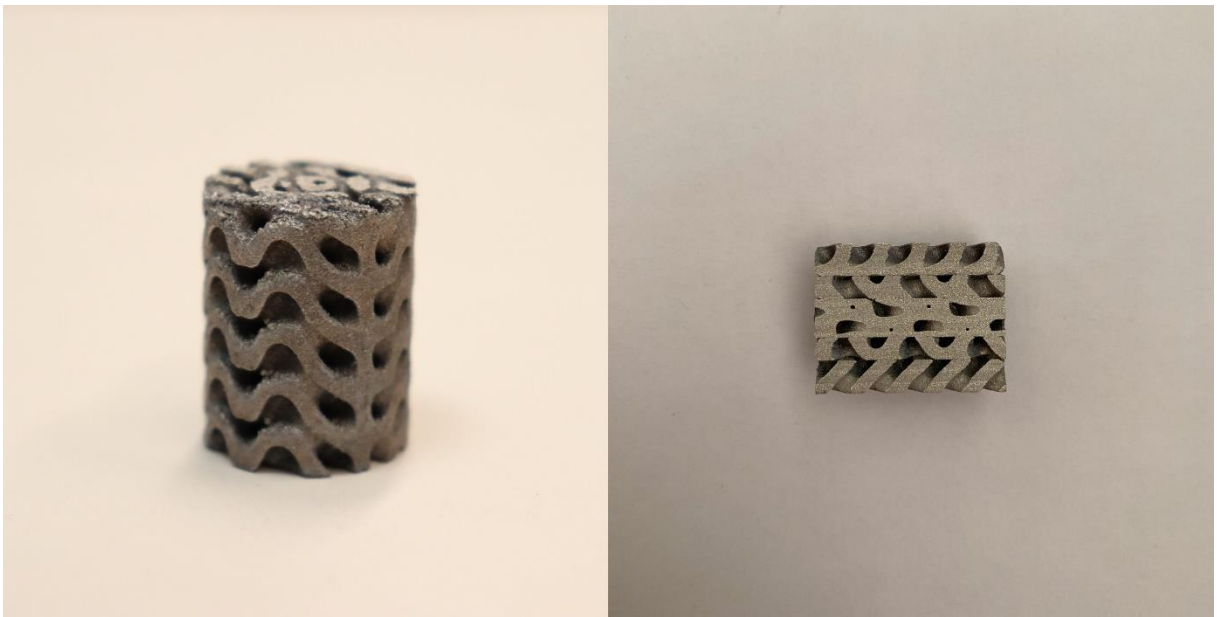
Figure 70. Surface images of 1st sample

Figure 71. Surface images of 2nd sample

Figure 72. Surface images of 3rd sample

Figure 73.Surface images of 4th sample
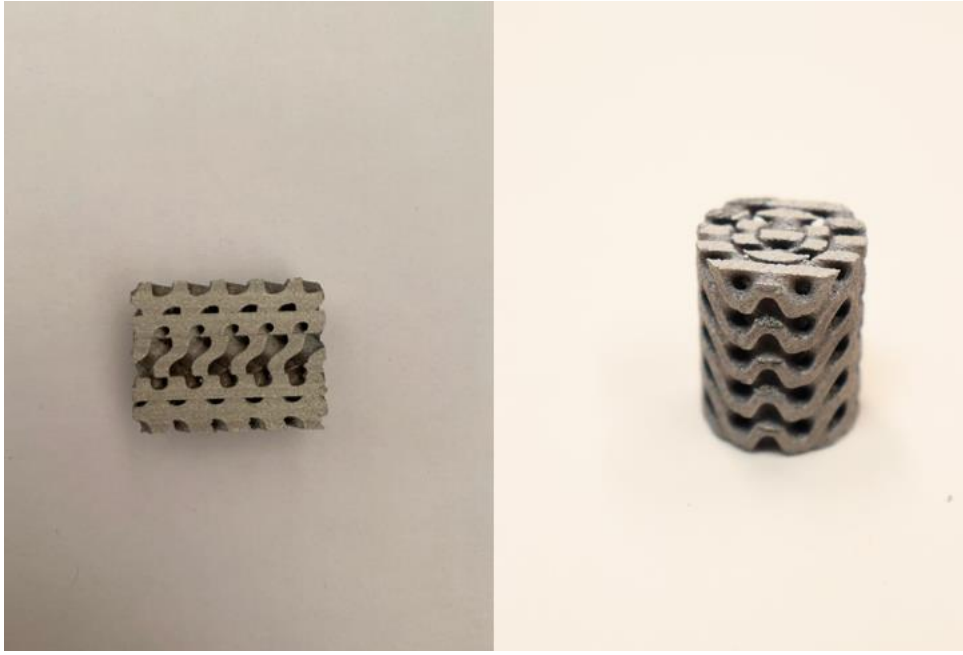
Figure 74. Surface images of 5th sample
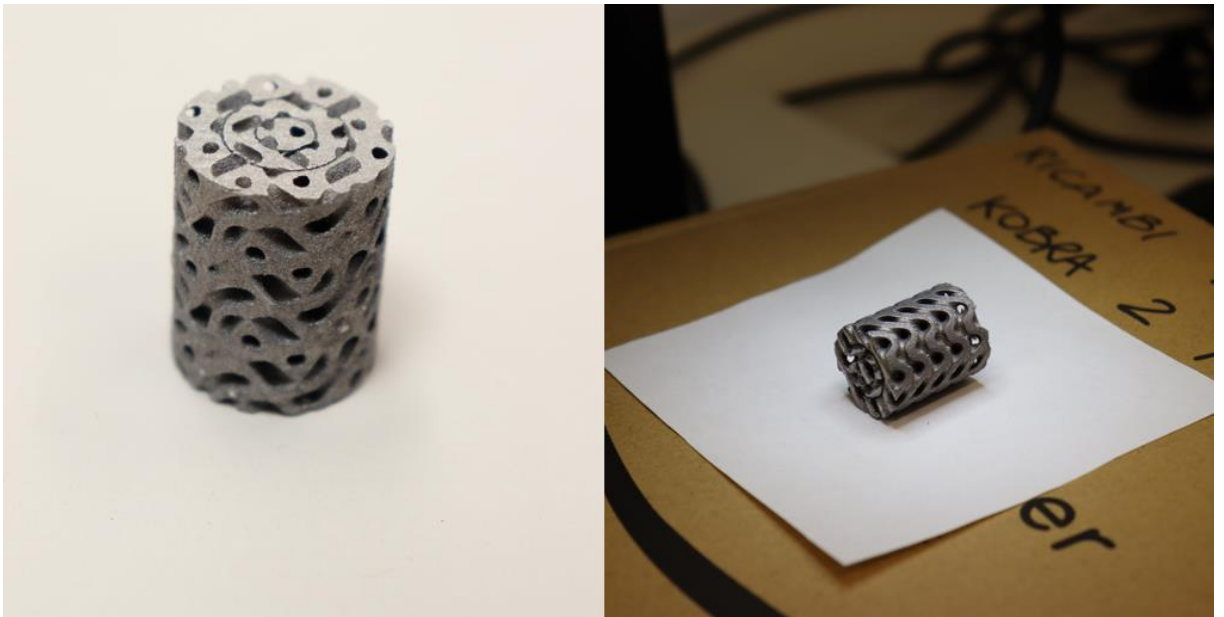
Figure 75. Surface images of 6th sample

8. REFERENCES

1. Selective electron beam manufactured Ti-6Al-4V lattice structures for orthopedic implant applications: Current status and outstanding challenges

2. Radial gradient design enabling additively manufactured low-modulus gyroid tantalum structures

3. Additive manufacturing and mechanical testing of functionally-graded steel strut-based lattice structures

4. Crushing response of triply periodic minimal surface structures fabricated by investment casting and powder bed fusion method

5. Caiazzo F, Alfieri V, Bujazha BD. Additive manufacturing of biomorphic scaffolds for bone tissue engineering. Int J Adv Manuf Technol 2021;113:2909–23. https://doi.org/10.1007/s00170-021-06773-5

6. Dehghan-Manshadi A, Venezuela J, Demir AG, Ye Q, Dargusch MS. Additively manufactured fe-35Mn-1Ag lattice structures for biomedical applications. J Manuf Process 2022;80:642–50. https://doi.org/10.1016/j.jmapro.2022.06.010.

7. Manzini BM, Machado LMR, Noritomi PY, da Silva JVL. Advances in bone tissue engineering: a fundamental review. J Biosci 2021;46:17. https://doi.org/10.1007/s12038-020-00122-6.

8. A mechanical property evaluation of graded density Al-Si10-Mg lattice structures manufactured by selective laser melting

9. https://www.eos.info/en/additive-manufacturing/3d-printing-metal/dmls-metal-materials

10. I. Gibson, D. W. Rosen, and B. Stucker, Additive Manufacturing Technologies: Rapid Prototyping to Direct Digital Manufacturing, 1st ed. Springer Publishing Company, Incorporated, 2009.

11. Master thesis (Correlation between the productivity and mechanical performance of AISI 316L parts produced via Laser powder bed fusion process)

12. V. Bhavar, P. Kattire, V. Patil, S. Khot, K. Gujar, and R. Singh, "A review on powder bed fusion technology of metal additive manufacturing," 2014.

13. Ashby, Michael F., and Lorna J. Gibson. "Cellular solids: structure and properties." *Press Syndicate of the University of Cambridge, Cambridge, UK* (1997): 175-231.

14. Overview of Methods and Software for the Design of Functionally Graded Lattice Structures

15. Xu, Zhuo, Seyed Mohammad Javad Razavi, and Majid R. Ayatollahi. "00019 Functionally Graded Lattice Structures: Fabrication Methods, Mechanical Properties, Failure Mechanisms and Applications." *International Journal of Impact Engineering* 125 (2022): 163-172.

16. Mechanical properties of functionally graded hierarchical bamboo structures T. Tan a,b , N. Rahbar c , S.M. Allameh d , S. Kwofie e , D. Dissmore a,b , K. Ghavami f , W.O. Soboyejo b,g,⇑

17. A review of recent research on bio-inspired structures and materials for energy absorption applications

18. Additively Manufactured Functionally Graded Lattices: Design, Mechanical Response, Deformation Behavior, Applications, and Insights

19. S. Rajagopalan, R.A. Robb, Schwarz meets Schwann: design and fabrication of biomorphic and durataxic tissue engineering scaffolds, Med. Image Anal. 10 (5) (2006) 693–712.

20. Continuous graded Gyroid cellular structures fabricated by selective laser melting: Design, manufacturing and mechanical properties

21. C. Yan, L. Hao, A. Hussein, S.L. Bubb, P. Young, D. Raymont, Evaluation of light-weight AlSi10Mg periodic cellular lattice structures fabricated via direct metal laser sintering, J. Mater. Process. Technol. 214 (4) (2014) 856–864.

22. C. Yan, L. Hao, A. Hussein, P. Young, Ti-6Al-4V triply periodic minimal surface structures for bone implants fabricated via selective laser melting, J. Mech. Behav. Biomed. Mater. 51 (2015) 61–73.

23. L. Yang, C. Yan, Y. Shi, Fracture Mechanism Analysis of Schoen gyroid Cellular Structures Manufactured by Selective Laser Melting, Solid Freeform Fabrication Symposium, 2017 2319–2325.

24. Master thesis Mechanical characterization of lattice structures manufactured by Selective Laser Melting process (SLM)

25. Zadpoor, Amir A. "Mechanical performance of additively manufactured meta-biomaterials." Acta biomaterialia 85 (2019): 41-59.Mahmoud, Dalia, et al. "Enhancement of heat exchanger performance using additive manufacturing of gyroid lattice structures." *The International Journal of Advanced Manufacturing Technology* 126.9 (2023): 4021-4036.

26. Bobbert, F. S. L., et al. "Additively manufactured metallic porous biomaterials based on minimal surfaces: A unique combination of topological, mechanical, and mass transport properties." *Acta biomaterialia* 53 (2017): 572-584.

27. Rezapourian, Mansoureh, et al. "Selective laser melted Ti6Al4V split-P TPMS lattices for bone tissue engineering." *International Journal of Mechanical Sciences* 251 (2023): 108353.

28. M. F. Ashby, "The properties of foams and lattices.," Philos. Trans. Ser. A, Math. Phys. Eng. Sci., vol. 364, no. 1838, pp. 15–30, Jan. 2006, doi: 10.1098/rsta.2005.1678.

29. Maskery, Ian, et al. "A mechanical property evaluation of graded density Al-Si10-Mg lattice structures manufactured by selective laser melting." Materials Science and Engineering: A 670 (2016): 264-274.

30. Yang, Lei, et al. "Continuous graded Gyroid cellular structures fabricated by selective laser melting: Design, manufacturing and mechanical properties." *Materials & Design* 162 (2019): 394-404.

31. Maskery, Ian, et al. "Compressive failure modes and energy absorption in additively manufactured double gyroid lattices." *Additive Manufacturing* 16 (2017): 24-29.

32. Caiazzo, Fabrizia, et al. "Metal functionally graded gyroids: additive manufacturing, mechanical properties, and simulation." *The International Journal of Advanced Manufacturing Technology* 123.7 (2022): 2501-2518.

33. Hussain, Sajjad, et al. "Effect of additive manufactured hybrid and functionally graded novel designed cellular lattice structures on mechanical and failure properties." *The International Journal of Advanced Manufacturing Technology* 128.11-12 (2023): 4873-4891.

34. Li, Baohua, and Richard M. Aspden. "Composition and mechanical properties of cancellous bone from the femoral head of patients with osteoporosis or osteoarthritis." Journal of bone and mineral research 12.4 (1997): 641-651.

35. Zhang, X. Z., et al. "Selective electron beam manufactured Ti-6Al-4V lattice structures for orthopedic implant applications: Current status and outstanding challenges." *Current Opinion in Solid State and Materials Science* 22.3 (2018): 75-99.

36. Wang, Jincheng, et al. "Understanding melt pool characteristics in laser powder bed fusion: An overview of single-and multi-track melt pools for process optimization." *Advanced Powder Materials* 2.4 (2023): 100137.

37. A.V. Gusarov, I. Yadroitsev, P. Bertrand, I. Smurov, Heat transfer modelling and stability analysis of selective laser melting, Appl. Surf. Sci. 254 (2007) 975–979.

38. Del Guercio, Giuseppe, Manuela Galati, and Abdollah Saboori. "Innovative approach to evaluate the mechanical performance of Ti–6Al–4V lattice structures produced by electron beam melting process." Metals and Materials International 27 (2021): 55-67.

39. Lannunziata, Erika, et al. "Laser powder bed fusion of AISI 316L lattice structures for biomedical applications." *Materials Today: Proceedings* 70 (2022): 345-351.

40. Pais, Ana, et al. "Multiscale Homogenization Techniques for TPMS Foam Material for Biomedical Structural Applications." *Bioengineering* 10.5 (2023): 515.

41. Zhang, Mingkang, et al. "Compressive behavior of hollow triply periodic minimal surface cellular structures manufactured by selective laser melting." *Rapid Prototyping Journal* 29.3 (2023): 569-581.

42. Ji, Weiming, et al. "Recent progress in gradient-structured metals and alloys." *Progress in Materials Science* (2023): 101194.

43. Bansal, Suneev Anil, Virat Khanna, and Pallav Gupta, eds. *Metal Matrix Composites: Fabrication, Production and 3D Printing*. CRC Press, 2022.

44. Polley, C., et al. "Morphological and mechanical characterisation of three-dimensional gyroid structures fabricated by electron beam melting for the use as a porous biomaterial." Journal of the Mechanical Behavior of Biomedical Materials 125 (2022): 104882.

45. Novak, Nejc, et al. "Quasi-static and dynamic compressive behaviour of sheet TPMS cellular structures." *Composite structures* 266 (2021): 113801.

46. Wakjira, Yosef, Arturo Cioni, and Hirpa G. Lemu. "Current status of the application of additive-manufactured TPMS structure in bone tissue engineering." *Progress in Additive Manufacturing* (2024): 1-18.

47. A. Salmi, Department of Management and production (DIGEP), Politecnico di Torino, Additive Manufacturing, 2023

48. Master's Degree Thesis Characterization of Inconel 718 fabricated by Selective Laser Melting (SLM) to achieve more productive parameters

49. Rometsch, Paul A., et al. "Review of high-strength aluminium alloys for additive manufacturing by laser powder bed fusion." *Materials & Design* 219 (2022): 110779.

50. https://www.primaadditive.com/en/materials/powder-bed-fusion/aluminium-alloys-pbf